



Boundary Conditions For the Extended Suture Model

by

Aneela Naheed

A dissertation submitted in partial fulfillment of the requirements
for the degree of Master of Philosophy in Physics

Supervised by


Dr. Asghar Qadir

School of Natural Sciences (SNS)

National University of Sciences and Technology
Islamabad, Pakistan

National University of Sciences & Technology**MS THESIS WORK**

We hereby recommend that the dissertation prepared under our supervision by: MS. Aneela Naheed, Regn No. 00000117074 Titled: Boundary Condition For Extended Suture Model be accepted in partial fulfillment of the requirements for the award of **MS** degree.

Examination Committee Members1. Name: PROF. AZAD A. SIDDIQUISignature: 2. Name: DR. MUBASHER JAMILSignature: External Examiner: DR. AMER IQBALSignature: Supervisor's Name: PROF. ASGHAR QADIRSignature: 


Head of Department

07/12/18
Date

COUNTERSIGNEDDate: 07/12/18


Dean/Principal

THESIS ACCEPTANCE CERTIFICATE

Certified that final copy of MS thesis written by **Ms. Aneela Naheed** (Registration No. **00000117074**), of **School of Natural Sciences** has been vetted by undersigned, found complete in all respects as per NUST statutes/regulations, is free of plagiarism, errors, and mistakes and is accepted as partial fulfillment for award of MS/M.Phil degree. It is further certified that necessary amendments as pointed out by GEC members and external examiner of the scholar have also been incorporated in the said thesis.

Signature: Asghar Qadir

Name of Supervisor: Prof. Asghar Qadir

Date: 07/12/18

Signature (HoD): Q. Javed

Date: 07/12/18

Signature (Dean/Principal): A/ Q. Javed

Date: 07/12/18

Dedicated to my mother,
who valued my education above all else and always
supported me

Acknowledgements

All praises and thanks to Allah Almighty, the Originator of the seven heavens, Who enabled me to complete this humble task. Secondly, I would like to thank my supervisor Prof. Asghar Qadir who believed in me and always encouraged me to complete my thesis, my GEC members Prof. Azad Akhter Siddique and Dr. Mubasher Jamil who cooperated during my research phase and all the teachers whoever taught me in my life.

Abstract

An attempt to prove the conjecture of Penrose, that in a closed Universe the black hole singularity and final singularity are simultaneous, Qadir and Wheeler constructed a Suture model by connecting two sections of Friedmann Universes using a Schwarzschild suture. Since the open (or flat) Universe has no final singularity it has to be compactified to test the conjecture. This extension has been done in this thesis for the open and flat models.

Contents

1	Introduction	5
1.1	The Special Theory of Relativity	5
1.1.1	Galilean and Lorentz Transformations	6
1.2	The Consequences of SR	8
1.2.1	Time Dilation	8
1.2.2	Length Contraction	10
1.2.3	Simultaneity	11
1.2.4	Mass Variation	11
1.2.5	Energy-Mass Equivalence	14
1.3	The Four-vector Formulation	15
1.4	The Null Cone Structure	17
1.5	The General Theory of Relativity	18
1.5.1	The Principle of Equivalence	19
1.5.2	The Principle of General covariance	19
1.6	The Curvature Tensors and Scalar	19
1.7	The Geodesic Equation	21
1.8	Geodesic Deviation	23
1.9	The Einstein Field Equations	24
1.10	Cosmology	25
1.10.1	The Friedmann Models of the Universe	27
1.10.2	Closed Friedmann Universe	27
1.10.3	Flat Friedmann Universe	28
1.10.4	Open Friedmann Universe	29
2	Black Holes and Their Singularities	30
2.1	The Schwarzschild Black Hole	32
2.1.1	Singularities of the Schwarzschild Black Hole	34
2.1.2	Eddington-Finkelstein Coordinates	35

2.1.3	Kruskal Coordinates	36
2.1.4	Kruskal-Szekeres Coordinates	37
2.1.5	The Compactified Kruskal-Szekeres Coordinates	38
2.2	Reissner-Nördstrom Black Hole	39
2.3	Kerr Black Hole	41
2.4	Kerr-Newmann Black Hole	41
3	The Suture Model	43
3.1	The Schwarzschild Lattice Universe	46
3.1.1	Foliation of Schwarzschild Lattice Universe	46
3.1.2	Modification of Schwarzschild Lattice Universe	47
3.2	The Suture Model	49
3.2.1	Features of Suture Model	50
3.2.2	Parameters of Suture Model	50
3.2.3	Boundary Conditions of Suture Model	52
3.2.4	Calculation of the Mass Discrepancy of Suture Model	55
3.2.5	Foliation of Suture Model	57
4	The Extended Suture Models	59
4.1	Open Suture Model	60
4.1.1	Boundary Conditions for the Open Suture Model	63
4.1.2	Calculation of the Mass Discrepancy of the Open Suture Model	65
4.2	Flat Suture Model	69
4.2.1	Boundary Conditions for the Flat Suture Model	72
4.2.2	Calculation of the Mass Discrepancy of the Flat Suture Model	74
5	Conclusion	77

Preliminaries

*There once was a lady named bright
who traveled much faster than light
She left home one day
in a relative way
and returned the previous night*

The above limerick refers to a remarkable result of Einstein's special theory of relativity that anything traveling faster than the speed of light experiences time travel. To develop a better understanding of this result, I will explain this theory and the consequences thoroughly in this thesis. Here, I will start my discussion by giving a brief review of Newtonian physics. Generally, this term can be applied to all the physics up until the development of Relativity by Einstein. Newtonian physics involves all kind of problems related to the motions, speeds and forces etc experienced by a particle. The fundamental assumption of Newtonian physics about space and time was that the time is a universal constant and it does not change with the relative motion of the observers. No doubt, Newtonian physics has its own charm in a sense that it leads us to the industrial revolution, developed a better understanding of the modern world, predicted and led to the discovery of Uranus, Neptune, Pluto and other astronomical bodies, but Einstein had tried a very different approach. He actually was interested in chasing a beam of light and exploring about the mysteries of the Universe. In 1905, he gave a revolutionary theory which explains the relative motion of the observers and the consistency of the speed of light. In the first chapter of this thesis, I shall briefly explain about the Special theory of relativity, consequences of this theory in detail, the transformations and notations applied to this theory. Since the motion of a particle is not restricted to one direction at a constant speed, therefore to study accelerated motion, Einstein generalized

his Special theory of relativity to the General theory by including gravity. I shall explain this theory in detail but to explain the concept of General relativity, it is necessary to give a brief review of differential geometry and a little about tensor notation. General relativity basically opened a gateway to the mysteries of the Universe. It enlightened the scientific world with many interesting phenomena including gravitational lensing, perihelion shift of Mercury, black holes and sciences like Astrophysics and Cosmology.

In the second chapter, I shall explain black holes in detail along with their singularities and the coordinates used to remove these singularities. This chapter involves all the basics of black holes necessary to develop an understanding of my research work. In the 3rd chapter, I shall review the work of Qadir and Wheeler on the Suture model for a closed Friedmann Universe. Before discussing this model, I shall explain some terminology and present other cosmological models. This chapter also includes the dynamics of the Suture Model, its boundary conditions and the evaluation of mass of black hole observed from the junction between the closed Friedmann Universe and the Schwarzschild geometry during the whole expansion of the model. At the end of the chapter, I shall give an idea about foliation of Suture Model. Although my research work is not related to the foliation but to arrive at the conclusion, it is necessary to mention about it. In the fourth chapter, I shall explain my research work in detail which is related to the extension of the Suture Model, to the open and flat Friedmann Universe. The basic point is that the open and flat Universe is limitless, therefore, in order to construct a model, I need to compactify it first. I will explain compactification, followed by the transformation of coordinates. The last chapter will consist of the conclusion of my thesis.

Chapter 1

Introduction

In the history of scientific revolution, many philosophers and scientists held different views regarding the concept of space and time. Aristotelian physics [1] introduced the concept of relativity. Aristotle believed that space is relative to its matter content and time to the chronology of events. In the 17th century, Newtonian mechanics [2] brought in a new concept of absoluteness of space and time. From the 17th to the 20th century, space and time were thought to be absolute quantities. Space was considered as a stage where events unfold and the location of a point was defined by a set of three coordinates (x, y, z) . Time, according to the Newtonian concept, was believed to be a universal entity that flows equally for all observers in the Universe, irrespective of their motion. Until the 19th century, space and time were two unconnected entities and there was no concept of defining them as a single entity, *spacetime*.

1.1 The Special Theory of Relativity

In 1905, Albert Einstein proposed a revolutionary theory that modified the Newtonian concept of space and time. Einstein's view was that space and time are not absolute quantities but they depend on the motion of the observers. He believed that the Universe can be visualized as a 4 dimensional continuum with 3 spatial and 1 time coordinate. Einstein's special theory of relativity (SR) is based on the following two principles:

(1) *The laws of physics are the same for all observers moving in an inertial frame of reference;*

(2) *The speed of light in a vacuum is constant for all observers regardless of their motion relative to the light source.*

The frame of reference in which Newton's second law of motion holds is called an inertial or non-accelerated frame of reference. As SR deals with uniform motion, it is also known as the "restricted theory of relativity".

1.1.1 Galilean and Lorentz Transformations

Before discussing the consequences of SR, it is necessary to mention Galilean and Lorentz transformations. In classical physics, Galilean transformations are used to transform the coordinates from one inertial frame of reference to another. Suppose that there are two frames of reference $O(t, x, y, z)$ and $O'(t', x', y', z')$ such that $O'(t', x', y', z')$ is moving with a velocity \mathbf{v} in the x -direction relative to $O(t, x, y, z)$. The equations that relate these two frames are:

$$t' = t, \quad x' = x - vt, \quad y' = y, \quad z' = z. \quad (1.1)$$

The Lorentz transformations are linear coordinate transformations that relate two coordinate frames moving at constant velocity relative to each other. To derive them, let us consider two frames of reference i.e $O(t, x, y, z)$ and $O'(t', x', y', z')$ such that at $t = t' = 0$, their origins coincide. At this instant, suppose that two light signals are sent by the observers in their respective frames which travels in both positive and negative x -axis at the same time [3]. The light signal proceeding along the positive x -axis for an observer in $O(t, x, y, z)$ is transmitted according to the equation

$$ct - x = 0, \quad (1.2)$$

while for an observer $O'(t', x', y', z')$, the equation will be of the form

$$ct' - x' = 0. \quad (1.3)$$

Since the speed of light is same for all observers, Eq.(1.2) and Eq.(1.3) can be related as

$$ct' - x' = \lambda(ct - x). \quad (1.4)$$

Similarly, by applying the same considerations to the light rays which are being transmitted along negative x -axis, we get

$$ct' + x' = \mu(ct + x), \quad (1.5)$$

where λ and μ are the constants of proportionality. Adding Eq.(1.4) and (1.5) and dividing by 2 we get,

$$ct' = \left(\frac{\lambda + \mu}{2}\right)ct - \left(\frac{\lambda + \mu}{2}\right)x, \quad (1.6)$$

where,

$$a = \frac{\lambda + \mu}{2} \quad ; \quad b = \frac{\lambda - \mu}{2}, \quad (1.7)$$

hence, Eq.(1.6) becomes

$$ct' = act - bx. \quad (1.8)$$

Subtracting Eq.(1.4) and Eq.(1.5) and dividing by 2

$$x' = -bct + ax. \quad (1.9)$$

Now, to find the solution of Eq.(1.8) and Eq.(1.9), we need to determine the value of a and b . The position of $O'(t', x', y', z')$ according to $O(t, x, y, z)$ is $x = vt$ while for $O'(t', x', y', z')$, $x' = 0$. Putting this value in Eq.(1.9), we get

$$b = av/c. \quad (1.10)$$

We can rewrite Eq.(1.8) and Eq.(1.9) in terms of b as

$$ct' = a\left(ct - \frac{v}{c}x\right), \quad (1.11)$$

$$x' = a\left(x - \frac{v}{c}ct\right). \quad (1.12)$$

To proceed further, all we have to do is to determine the value of a . Since at the beginning of time, both the observer are at rest position. For this purpose, let $x = x_0$ at $t = 0$, such that the Eq.(1.12) becomes

$$\frac{x_0}{x'} = \frac{1}{a}. \quad (1.13)$$

Similarly for $t' = 0$, consider x' as x_0 and put it in Eq.(1.11) to get

$$ct = \frac{v}{c}x. \quad (1.14)$$

Putting the value of ct in Eq.(1.12), we have

$$x'_0 = a\left(x - \frac{v^2}{c^2}x\right). \quad (1.15)$$

After solving the above equation, we get

$$\frac{x'_0}{x} = a\left(1 - \frac{v^2}{c^2}\right). \quad (1.16)$$

The first principle of SR implies that

$$\frac{x_0}{x'} = \frac{x'_0}{x}, \quad (1.17)$$

which can be further written as

$$\frac{x_0}{x'} = a\left(1 - \frac{v^2}{c^2}\right). \quad (1.18)$$

Inserting this value in Eq.(1.13), we get

$$a = \frac{1}{\sqrt{1 - \frac{v^2}{c^2}}}. \quad (1.19)$$

Putting the values of a , b in Eq.(1.11) and Eq.(1.12), we get

$$t' = \gamma(t - vx/c^2), \quad x' = \gamma(x - vt), \quad y' = y, \quad z' = z, \quad (1.20)$$

where,

$$a = \gamma = \frac{1}{\sqrt{1 - \beta^2}} \quad ; \quad \beta = v/c.$$

Galileon transformation are not much effective if the speed of an object become very large such that it approaches to the speed of light while in classical limit, Lorentz transformation reduces to Galilean transformation.

1.2 The Consequences of SR

SR includes the following consequences which had been tested and verified experimentally:

1.2.1 Time Dilation

Let δt be the time interval as measured by an observer in a rest frame $O(x, y, z, t)$ where the position of an observer remains the same i.e $x_2 = x_1$.

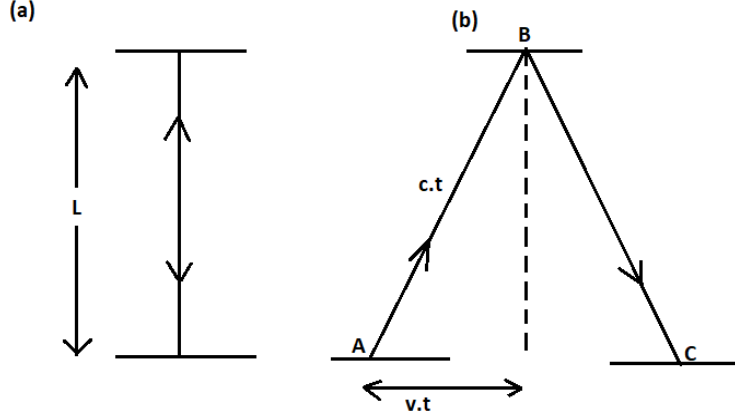


Figure 1.1: The time dilation phenomenon measured for stationary and moving photon clocks.

The time interval measured in a moving frame $O'(x', y', z', t')$ can be calculated by using Eq.(1.20).

$$t'_1 = \gamma(t_1 - \frac{vx_1}{c^2}), \quad (1.21)$$

$$t'_2 = \gamma(t_2 - \frac{vx_2}{c^2}), \quad (1.22)$$

$$\delta t' = t'_1 - t'_2 = \gamma \delta t. \quad (1.23)$$

The above equation expresses the fact that the units of measurement of a time interval for a moving frame is larger than that of a stationary frame. In other words, a moving clock ticks slower as compared to a stationary clock, so we can say that the time dilates for a moving observer. The time dilation effect is more significant for relativistic motions such that the flow of time ceases completely for the particles moving with the speed of light (classically impossible). The following experiment explains this phenomenon in an elegant way [4].

Let us consider a photon clock consisting of two mirrors attached on the top and bottom of it, separated by a distance L . In a fixed frame, a beam of light moves from the lower to the top mirror, reflected and returns back to the lower mirror. The time taken by the light beam is $\Delta t = \frac{2L}{c}$ where Δt is called the proper time as measured by an observer at rest with respect to the clock. Now suppose that this observer starts moving at velocity \mathbf{v} with

respect to a stationary observer. The light beam, in this case, will follow a triangular path as it moves from lower to the top mirror as depicted in Figure 1.1. The time measured by a stationary observer between the two mirror is $\frac{\Delta t'}{2}$. According to the second observer, light ray travels a distance of $\frac{c\Delta t'}{2}$ and meanwhile, the clock moves a forward distance of $\frac{v\Delta t'}{2}$. Using Pythagora's theorem, we get

$$\left(\frac{c\Delta t}{2}\right)^2 + \left(\frac{v\Delta t'}{2}\right)^2 = \left(\frac{c\Delta t'}{2}\right)^2. \quad (1.24)$$

Solving for $\Delta t'$, we get

$$\Delta t' = \gamma\Delta t. \quad (1.25)$$

The above relation is called the time dilation formula.

1.2.2 Length Contraction

Another interesting consequence predicted by SR is the difference between measurement of length of an object with respect to a stationary and moving observer. Let δL be the proper length of a rod measured by an observer in a rest frame. Now consider that the observer takes the rod and start running, then the length of a rod measured by a stationary observer seems shorter which can be calculated by using Eq.(1.20). As the time interval in a moving frame is not changing therefore $t'_1 - t'_2 = 0$.

$$t_1 - t_2 = \frac{v}{c^2}(L_1 - L_2). \quad (1.26)$$

Therefore,

$$\delta L' = L'_1 - L'_2, \quad (1.27)$$

$$\delta L' = \gamma((L_1 - L_2) - v(t_1 - t_2)), \quad (1.28)$$

$$\delta L' = \gamma\delta L\left(1 - \frac{v^2}{c^2}\right), \quad (1.29)$$

$$\delta L' = \frac{\delta L}{\gamma}. \quad (1.30)$$

This relation is known as the length contraction formula which states that the length of a moving object appears shorter than its original length from the perspective of a stationary observer.

1.2.3 Simultaneity

Simultaneity is an important concept in SR which states that inertial observers in relative motion disagree on the timing of events occurring at different places, i.e. if an event occurring at two different points x_1 and x_2 appears simultaneous to an observer $O(t, x, y, z)$, it is not necessarily simultaneous for another observer $O'(t', x', y', z')$ which is moving relative to the first. This fact can be illustrated by the following thought experiment. Consider a man standing at the midpoint of a platform observing a flash of light hitting the ground at either side of him. Let the left side of a man be labeled A and the right side B. According to the man, light hits the ground at the same time, i.e, the two events happened simultaneously. Now consider, there is a lady sitting on a train which is moving relative to the platform along with its length. From the perspective of the lady, the platform moves rapidly in a direction from A towards B. If we observe the above phenomenon with respect to that lady, light strikes at A earlier than B. Thus the two events that appeared simultaneous to a man on the platform did not occur at the same time according to a lady sitting in the train. Mathematically, this effect can be formulated by considering two events happening at two different locations x_1 and x_2 . Suppose that the two event appears simultaneous to an observer $O(t, x, y, z)$ i.e, $t_1 = t_2$. According to another observer, $O'(t', x', y', z')$ moving relative to $O(t, x, y, z)$, the event occurs at

$$t'_1 = \gamma(t_1 - \frac{v}{c^2}x_1), \quad (1.31)$$

$$t'_2 = \gamma(t_2 - \frac{v}{c^2}x_2), \quad (1.32)$$

since $t_1 = t_2 = t$, this implies

$$t'_1 - t'_2 = \gamma \frac{v}{c^2}(x_2 - x_1). \quad (1.33)$$

As $x_2 \neq x_1$, this implies that simultaneity is not absolute rather it is relative. The most general misconception about Special Theory of Relativity is the belief that according to this theory, everything is relative but it is just the motion and simultaneity that is taken to be relative [5].

1.2.4 Mass Variation

According to SR, the mass of an object in a stationary frame, called the rest mass denoted by m_o is not a constant quantity with respect to an observer in

a moving frame of reference. To derive a relation between rest mass m_o and the relativistic mass m (mass in a moving frame), let us consider two inertial frames of reference O and O' . O is stationary while O' is moving relative to O in x -direction. Consider two masses m_1 and m_2 in a O' moving with same velocity towards each other i.e u and $-u$. According to the velocity-addition theorem

$$u_1 = \frac{u + v}{1 + \frac{uv}{c^2}}. \quad (1.34)$$

Similarly, for mass m_2 , the velocity will be

$$u_2 = \frac{-u + v}{1 - \frac{uv}{c^2}}. \quad (1.35)$$

Now, both the masses approaches to each other, collide and after collision, they move apart. Applying law of conservation of momentum, i.e.

Momentum before collision = Momentum after collision

$$m_1 u_1 + m_2 u_2 = (m_1 + m_2)v. \quad (1.36)$$

Substituting Eq.(1.34) and Eq.(1.35) in above equation, we get

$$m_1 \left[\frac{u + v}{1 + \frac{uv}{c^2}} \right] + m_2 \left[\frac{-u + v}{1 - \frac{uv}{c^2}} \right] = (m_1 + m_2)v. \quad (1.37)$$

Combining m_1 and m_2 terms, we get

$$m_1 \left[\frac{u + v}{1 + \frac{uv}{c^2}} - v \right] = m_2 \left[v - \frac{-u + v}{1 - \frac{uv}{c^2}} \right]. \quad (1.38)$$

After simplifying the above equation, we get

$$m_1 \left[\frac{c^2 u - uv^2}{c^2 + uv} \right] = m_2 \left[\frac{c^2 u - uv^2}{c^2 - uv} \right]. \quad (1.39)$$

Re-arranging the above equation, we get

$$\frac{m_1}{m_2} = \frac{\left[\frac{c^2 u - uv^2}{c^2 + uv} \right]}{\left[\frac{c^2 u - uv^2}{c^2 - uv} \right]}. \quad (1.40)$$

Simplifying, we get

$$\frac{m_1}{m_2} = \frac{1 + \frac{uv}{c^2}}{1 - \frac{uv}{c^2}}. \quad (1.41)$$

Now, squaring Eq.(1.34), dividing by c^2 and adding 1 on both sides, we get

$$\frac{u_1^2}{c^2} + 1 = \left(\frac{u + v}{c^2 \left(1 + \frac{uv}{c^2}\right)} \right)^2 + 1, \quad (1.42)$$

the above equation can also be written as

$$1 - \frac{u_1^2}{c^2} = 1 - \left(\frac{u + v}{c^2 \left(1 + \frac{uv}{c^2}\right)} \right)^2. \quad (1.43)$$

Simplifying the right side of the above equation, we get

$$1 - \frac{u_1^2}{c^2} = \frac{(1 - \frac{v^2}{c^2})(1 - \frac{v^2}{c^2})}{(1 + \frac{uv}{c^2})^2}. \quad (1.44)$$

Similarly, for m_2 , the relation is given by

$$1 - \frac{u_2^2}{c^2} = \frac{(1 - \frac{v^2}{c^2})(1 - \frac{v^2}{c^2})}{(1 - \frac{uv}{c^2})^2}. \quad (1.45)$$

Dividing Eq.(1.44) and Eq.(1.45), we get

$$\frac{1 - \frac{u_2^2}{c^2}}{1 - \frac{u_1^2}{c^2}} = \frac{(1 + \frac{uv}{c^2})^2}{(1 - \frac{uv}{c^2})^2}. \quad (1.46)$$

Taking square root and comparing it with Eq.(1.41), we get

$$\frac{m_1}{m_2} = \frac{\sqrt{1 - \frac{u_2^2}{c^2}}}{\sqrt{1 - \frac{u_1^2}{c^2}}}. \quad (1.47)$$

The above equation can be written as

$$m_1 \sqrt{1 - \frac{u_2^2}{c^2}} = m_2 \sqrt{1 - \frac{u_1^2}{c^2}} = m_o. \quad (1.48)$$

Therefore,

$$m_1 \sqrt{1 - \frac{u_2^2}{c^2}} = m_o. \quad (1.49)$$

Replacing m_1 with m and u_1 with v , we get

$$m = \frac{m_o}{\sqrt{1 - \frac{v^2}{c^2}}}. \quad (1.50)$$

The above relation is the mass variation relation which shows that mass of an object changes with the velocity, hence it is not a constant quantity.

1.2.5 Energy-Mass Equivalence

Another revolutionary consequence of SR includes the famous Einstein's mass energy equation $E = mc^2$, which states that the mass and energy are interconvertible. The body moving faster appears to gain weight and become heavier, as it approaches to the speed of light it converts in to energy. This relation can be derived by taking square on both sides of Eq.(1.50), we get

$$m^2 = \frac{m_o^2}{(1 - \frac{v^2}{c^2})}. \quad (1.51)$$

Simplifying the above equation, we get

$$m^2 c^2 - m^2 v^2 = m_o^2 c^2. \quad (1.52)$$

Taking the differentials on both sides, we get

$$2mc^2 dm - 2mv^2 dm - 2vm^2 dv = 0. \quad (1.53)$$

Simplifying further, we get

$$c^2 dm = v^2 dm + mvdv. \quad (1.54)$$

Now, the change in kinetic energy is equal to the change in the work done which is equal to the product of force and displacement, i.e,

$$dK = dW = Fds. \quad (1.55)$$

According to the Newton's second law of motion,

$$F = \frac{dP}{dt}, \quad (1.56)$$

where, momentum is equal to the product of mass and velocity. Putting value of P in Eq.(1.56), we get

$$F = \frac{d}{dt}(mv), \quad (1.57)$$

$$F = m \frac{dv}{dt} + v \frac{dm}{dt}. \quad (1.58)$$

Putting value of F in Eq.(1.55), we get

$$dK = m \frac{dv}{dt} . ds + v \frac{dm}{dt} . ds. \quad (1.59)$$

The above equation can be written as

$$dK = m \frac{ds}{dt} dv + v \frac{ds}{dt} dm. \quad (1.60)$$

As, $\frac{ds}{dt} = v$, therefore Eq.(1.60) reduces to

$$dK = mv dv + v^2 dm. \quad (1.61)$$

Comparing Eq.(1.54) and Eq.(1.61), we get

$$dK = c^2 dm. \quad (1.62)$$

Taking integrals on both sides with the limits 0 to K for dK and m_o to m for dm , we get

$$K = mc^2 - m_o c^2, \quad (1.63)$$

which can be re-written as

$$K + m_o c^2 = mc^2, \quad (1.64)$$

where, the term on left side represents the total energy of a particle, therefore, we get

$$E = mc^2. \quad (1.65)$$

Hence, we can conclude that the mass and energy are basically the same aspects of two different approaches.

1.3 The Four-vector Formulation

In 1907, Hermann Minkowski realized that SR, proposed by his former student, Albert Einstein, could be reformulated in a more mathematical way by using four-vectors. Einstein at first considered Minkowski's treatment merely as a mathematical trick, but later he realized that a geometrical view of spacetime is necessary for generalizing SR. A four-vector is a vector that

describes the position of an event in Minkowski spacetime. It is represented by x^μ consisting of 1 time and 3 space components.

$$x^\mu = (x^0, x^1, x^2, x^3).$$

To make the time component dimensionally consistent with the space component, we put $x^0 = ct$, such that

$$x^\mu = (ct, x, y, z).$$

A four-vector is invariant under the Lorentz transformations. Let us consider the two frames of reference O and O' . The coordinates measured in O are (ct, x, y, z) while the coordinates measured in O' are (ct', x', y', z') where, O' is moving with the velocity \mathbf{v} in x -direction relative to O . The Lorentz transformations in four-vector notation is given by,

$$x'^0 = \gamma(x^0 - \beta x^1) \quad , \quad x'^1 = \gamma(x^1 - \beta x^0) \quad , \quad x'^2 = x^2 \quad , \quad x'^3 = x^3. \quad (1.66)$$

In matrix form

$$\begin{bmatrix} x'^0 \\ x'^1 \\ x'^2 \\ x'^3 \end{bmatrix} = \begin{bmatrix} \gamma & -\gamma\beta & 0 & 0 \\ -\gamma\beta & \gamma & 0 & 0 \\ 0 & 0 & 1 & 0 \\ 0 & 0 & 0 & 1 \end{bmatrix} \begin{bmatrix} x^0 \\ x^1 \\ x^2 \\ x^3 \end{bmatrix}. \quad (1.67)$$

The above equation can be written in tensor notation as

$$x'^\mu = \sum_{v=0}^3 \Lambda_v^\mu x^v, \quad (1.68)$$

where,

$$\Lambda_v^\mu = \begin{bmatrix} \gamma & -\gamma\beta & 0 & 0 \\ -\gamma\beta & \gamma & 0 & 0 \\ 0 & 0 & 1 & 0 \\ 0 & 0 & 0 & 1 \end{bmatrix}.$$

This relation can be written by using Einstein's summation convention as

$$x'^\mu = \Lambda_v^\mu x^v. \quad (1.69)$$

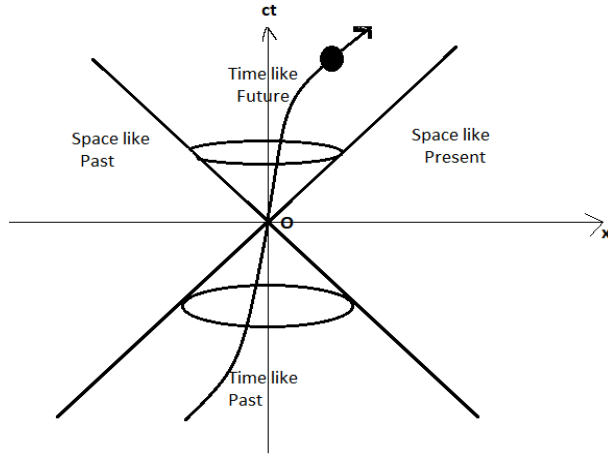


Figure 1.2: The space-time diagram of a null cone representing time-like, light-like and space-like regions.

1.4 The Null Cone Structure

The null cone, also known as a light cone, is a surface that describes the path of a flash of light originating from a single event and traveling in all directions through spacetime. A null cone structure divides the Four-vector dx^μ into three regions depending on the value of line element ds^2 as

$$ds^2 = g_{\mu\nu} dx^\mu dx^\nu. \quad (1.70)$$

There exist three kinds of vectors corresponding to the value of ds^2 , i.e.

$$ds^2 = c^2 dt^2 - \mathbf{dx} \cdot \mathbf{dx} > 0; \quad (1.71)$$

$$ds^2 = c^2 dt^2 - \mathbf{dx} \cdot \mathbf{dx} = 0; \quad (1.72)$$

$$ds^2 = c^2 dt^2 - \mathbf{dx} \cdot \mathbf{dx} < 0. \quad (1.73)$$

A four dimensional region which represents the interior of the null cone is given by the Eq.(1.71). All the vectors that lie inside this region are called time-like vectors, which represents the actual geodesics of a physical object traveling through spacetime. This region can be further divided into future-directed ($dx^0 > 0$) and past-directed ($dx^0 < 0$) subregions. Similarly a three dimensional surface representing the boundary of a null cone is given by

the Eq.(1.72) and the vectors lying in this region are called null, or light-like, vectors. Null vectors represent the path of an object traveling at the speed of light. Like time-like vectors, they are also subdivided in to future-directed and past-directed null vectors. The external structure of a null cone which consists of all the vectors that lie outside of a null cone representing the geodesic of a physical object traveling greater than the speed of light is given by the Eq.(1.73) and these vectors are known as space-like vectors. Time-like, space-like and null or light-like vectors are invariant under Lorentz transformations. The regions consisting of these vectors are shown in Figure 1.2.

1.5 The General Theory of Relativity

After presenting SR, which describes the uniform linear motion of an object restricted to the inertial frame of reference, Albert Einstein started working for the general case which involves the arbitrary motion of an object. It took Einstein ten years to include acceleration and generalize the special, or restricted theory from uniform linear motion to the arbitrary motion. This new theory of space, time and gravitation is known as the General Theory of Relativity (GR).

GR, published in 1915, is a geometric theory which propose that space-time is not a flat structure, but it can be distorted by the presence of massive objects that produces the curvature in spacetime. GR replaces the Newtonian gravitational force by the curvature of spacetime. In the 17th century Issac Newton proposed the law of Universal gravitation stated as: Every object in the Universe attracts every other object with a force \mathbf{F} which is directly proportional to the product of their masses and inversely proportional to the square of distance r between them [6]. Mathematically, it can be expressed as

$$\mathbf{F} = -\frac{GMm}{r^2}\hat{\mathbf{r}}, \quad (1.74)$$

where, \mathbf{F} is the force, M and m are the masses of the first and second object, G is the gravitational constant and r is the distance between the center of their masses. GR is based on the following principles:

1.5.1 The Principle of Equivalence

In November 1907, a thought broke into Einstein's mind which he later called "the happiest thought of his life". By imagining a man standing in an elevator freely falling under gravity, he realized that there must be some relation between inertia and gravitation. He concluded that the experiments performed in a uniformly accelerated frame of reference with acceleration \mathbf{a} are consistent with the experiments performed in a non-accelerated frame of reference situated in a gravitational field with the acceleration of gravity $\mathbf{g}=-\mathbf{a}$, i.e. acceleration is equivalent to the gravitation. In simple words, being stationary in a gravitational field or accelerating upward are the same things. The principle of equivalence is stated as

For an observer in free fall in a gravitational field, the results of all local experiments are independent of the magnitude of the gravitational field.

1.5.2 The Principle of General covariance

The principle of general covariance states that

The general laws of physics in a gravitational field are to be expressed by the equations that are invariant under any set of transformations [7]. These physical equations also hold in the absence of gravity.

1.6 The Curvature Tensors and Scalar

Before going in to the discussion of curvature tensors and scalar, it is necessary to mention about the covariant derivative. The coordinatization of the tensor, \mathbf{T} , obtained by acting on a contravariant vector, \mathbf{X} , with the affine connection is called the covariant derivative of \mathbf{X} , given by

$$T_b^a = X^a_{;b} = X^a_{,b} + \Gamma^a_{b\ c} X^c, \quad (1.75)$$

The covariant derivative of a covariant vector is evaluated by the following formula

$$X_{a;b} = X_{a,b} - \Gamma^c_{b\ a} X_c. \quad (1.76)$$

Gauss invariant intrinsic curvature of a surface can be generalized to a higher dimensional space by carrying a basis vector along two opposite directions in

opposite order and taking difference of the two results [8]. This can be done by using a covariant derivative.

$$X^a_{;c;d} - X^a_{;d;c} = (X^a_{,c} + \Gamma^a_{b\ c} X^b)_{;d} - (X^a_{,d} + \Gamma^a_{d\ b} X^b)_{;c}, \quad (1.77)$$

$$X^a_{;c;d} - X^a_{;d;c} = (\Gamma^a_{b\ c,d} - \Gamma^a_{d\ b,c}) X^b + (\Gamma^a_{c\ f} \Gamma^f_{d\ b} - \Gamma^a_{d\ f} \Gamma^f_{c\ b}) X^b, \quad (1.78)$$

$$X^a_{;c;d} - X^a_{;d;c} = \Gamma^a_{b\ c,d} - \Gamma^a_{d\ b,c} + \Gamma^a_{c\ f} \Gamma^f_{d\ b} - \Gamma^a_{d\ f} \Gamma^f_{c\ b}, \quad (1.79)$$

$$X^a_{;c;d} - X^a_{;d;c} = R^a_{bcd} X^b, \quad (1.80)$$

where,

$$R^a_{bcd} = \Gamma^a_{b\ c,d} - \Gamma^a_{d\ b,c} + \Gamma^a_{c\ f} \Gamma^f_{d\ b} - \Gamma^a_{d\ f} \Gamma^f_{c\ b}, \quad (1.81)$$

is called the Riemann curvature tensor that measures the curvature of space-time. If $R^a_{bcd} = 0$, it represents the Minkowski spacetime or we can say it is locally flat in some regions. The Christoffel symbol used in the above expression is given by the following formula

$$\Gamma^a_{b\ c} = \frac{1}{2} g^{ad} (g_{bd,c} + g_{cd,b} - g_{bc,d}). \quad (1.82)$$

The Riemann curvature tensor possesses the following properties:

1. R_{abcd} is skew-symmetric in the first two and last two indices, i.e.

$$R_{abcd} = -R_{bacd} = -R_{abdc}, \quad (1.83)$$

2. If both pairs of indices are interchanged, then it is symmetric

$$R_{abcd} = R_{cdab}. \quad (1.84)$$

3. It satisfies the first and second Bianchi identities given by

$$R_{abcd} + R_{acdb} + R_{adcb} = 0, \quad (1.85)$$

$$R^a_{bcd;e} + R^a_{bec;d} + R^a_{bde;c} = 0. \quad (1.86)$$

Contracting the first and third indices of Riemann curvature tensor yields the Ricci tensor while contracting Ricci tensor, we get Ricci scalar

$$R_{bd} = R^a_{bad}, \quad (1.87)$$

$$R = g^{bd} R_{bd}. \quad (1.88)$$

The Riemann tensor also determines the type of singularity present in spacetime. From the geometric point of view, the singularities are points where the metric becomes infinite and the geodesic becomes incomplete. There are generally two types of singularities in GR. Essential singularity, also known as the physical or spacetime singularity, arises when the curvature of spacetime becomes infinite. It is a region in spacetime where the gravitational field of an object is infinite to an extent that does not require any coordinate system. If a singularity can be removed by changing the coordinate system, then this kind of singularity is known as a coordinate singularity, which arises because of a bad choice of coordinates. The nature of singularity can also be found by the following four curvature invariants:

$$\begin{aligned}
R_1 &= R, \\
R_2 &= R_{cd}^{ab} R_{ab}^{cd}, \\
R_3 &= R_{cd}^{ab} R_{ef}^{cd} R_{ab}^{ef}, \\
R_4 &= R_{cd}^{ab} R_{ef}^{cd} R_{gh}^{ef} R_{ab}^{gh}.
\end{aligned} \tag{1.89}$$

If all the above curvature invariants are finite, then the singularity is coordinate, otherwise it is essential.

1.7 The Geodesic Equation

On a curved space, the shortest path between two points is called a *geodesic*. In Minkowski spacetime, the shortest distance between two points is the straight line. Using the Euler-Lagrange equations, the shortest path between two points can be found as

$$S_{AB} = \int_A^B ds, \tag{1.90}$$

$$S_{AB} = \int_A^B 1 \cdot ds, \tag{1.91}$$

where S is the arc length between two points A and B.

$$S_{AB} = \int_A^B L[x^a, \dot{x}^a] ds. \tag{1.92}$$

where, L , is a Lagrangian function that describes the state of a dynamic system in terms of position coordinates and their time derivatives and is equal to the difference of the kinetic and potential energy. The Euler-Lagrange equations are given by

$$\frac{\partial L}{\partial x^c} - \frac{d}{ds} \left(\frac{\partial L}{\partial \dot{x}^c} \right) = 0, \quad (1.93)$$

where,

$$\frac{\partial L}{\partial x^c} = g_{ab,c} \dot{x}^a \dot{x}^b, \quad (1.94)$$

$$\frac{\partial L}{\partial \dot{x}^c} = g_{cb} \dot{x}^b + g_{ac} \dot{x}^a, \quad (1.95)$$

$$\frac{d}{ds} \left(\frac{\partial L}{\partial \dot{x}^c} \right) = (g_{ac,d} \dot{x}^a + g_{cb,d} \dot{x}^b) \dot{x}^d + g_{dc} \ddot{x}^d + g_{cd} \ddot{x}^d. \quad (1.96)$$

Putting the above values in Euler-Lagrange equation, we get

$$g_{ab,c} \dot{x}^a \dot{x}^b + (g_{ac,d} \dot{x}^a + g_{cb,d} \dot{x}^b) \dot{x}^d + 2g_{cd} \ddot{x}^d = 0. \quad (1.97)$$

Replacing the dummy index “d” by “b” in the second term and “d” by “a” in the third term, we get

$$2g_{cd} \ddot{x}^d + (g_{ac,b} + g_{bc,a} + g_{ab,c}) \dot{x}^a \dot{x}^b = 0, \quad (1.98)$$

$$g_{cd} \ddot{x}^d + \frac{1}{2} (g_{ac,b} + g_{bc,a} + g_{ab,c}) \dot{x}^a \dot{x}^b = 0, \quad (1.99)$$

$$\ddot{x}^d + \Gamma_{bc}^a \dot{x}^a \dot{x}^b = 0. \quad (1.100)$$

The above equation is known as the *geodesic equation* and solution of this equation is called a *geodesic*.

Lie Derivative

In differential geometry, there are two ways of taking derivative of a tensor along a curve, which are invariant under the coordinate transformations. One is to ignore the effect of the coordinatization on the tensor and apply the derivation to the tensor. This is called the intrinsic derivative. The other way is to pull out the effect of the coordinatization of the tensor and compute the effect of the derivation on the tensor in the manifold. This is called the Lie derivative.

For a general tensor with components $X^{a\dots c}{}_{d\dots f}$, the Lie derivative is given by

$$\begin{aligned} (\mathcal{L}_t X)^{a\dots c}{}_{d\dots f} &= t^p X^{a\dots c}{}_{d\dots f,p} - X^{p\dots c}{}_{d\dots f} t^a{}_{,p} - \dots \\ &- X^{a\dots p}{}_{d\dots f} t^c{}_{,p} + X^{a\dots c}{}_{p\dots f} t^p{}_{,d} + X^{a\dots c}{}_{d\dots p} t^p{}_{,f}. \end{aligned} \quad (1.101)$$

Lie and Parallel Transport

If the tensor is displaced parallelly in the coordinate system. This is called the parallel transport, instead, if the tensor is displaced along the curve on the manifold by using a Lie derivative. This is called Lie transport.

1.8 Geodesic Deviation

Let us consider two neighboring geodesics connected by the separation vector \mathbf{v} while the tangent vectors along their geodesics are \mathbf{t} . For a separation vector \mathbf{v} to be transported parallel along the curve, it is necessary that

$$\mathcal{L}_t v^a = 0, \quad (1.102)$$

where \mathcal{L} is a Lie derivative along the curve. Using the definition of Lie derivative, we get

$$t^d v^a{}_{;d} - v^d t^a{}_{;d} = 0, \quad (1.103)$$

$$t^d v^a{}_{;d} = v^d t^a{}_{;d}. \quad (1.104)$$

Geodesic deviation is given by the acceleration vector A , as

$$A^a = \frac{d^2 v^a}{ds^2}, \quad (1.105)$$

$$A^a = t^c [t^d v^a{}_{;d}]_{;c}. \quad (1.106)$$

By using Eq.(1.104), we get

$$A^a = t^c [v^d t^a{}_{;d}]_{;c}, \quad (1.107)$$

$$A^a = t^c v^d{}_{;c} t^a{}_{;d} + t^c v^d t^a{}_{;d;c}, \quad (1.108)$$

$$A^a = v^c t^d{}_{;c} t^a{}_{;d} + t^c v^d t^a{}_{;d;c}, \quad (1.109)$$

$$A^a = v^c (t^d t^a{}_{;d})_{;c} - v^c t^d t^a{}_{;d;c} + t^c v^d t^a{}_{;d;c}, \quad (1.110)$$

Simplifying the above equation, we get

$$A^a = t^c v^d t^a_{;d;c} + v^c t^d t^a_{;d;c}. \quad (1.111)$$

Interchanging “c” and “d” in the first term, we get

$$A^a = t^d v^c t^a_{;c;d} + v^c t^d t^a_{;d;c}, \quad (1.112)$$

$$A^a = R^a_{bcd} t^b v^c t^d. \quad (1.113)$$

The above equation represents that acceleration arises due to the curvature of spacetime.

1.9 The Einstein Field Equations

The Einstein field equations are the set of 10 non-linear partial differential equations which represents the relationship between curvature and matter distribution of spacetime. GR deals with the gravitational fields depending on the distribution of matter and its evolution [8]. All the stresses, energy and momentum in spacetime can be represented mathematically by a tensor known as the *Stress-energy momentum tensor*, T^{ab} given by

$$T^{ab} = \rho u^a u^b \sigma^{ij} \delta_i^a \delta_j^b, \quad (1.114)$$

where, ρ is the density u^a is the four-velocity and σ^{ij} is called the stress-tensor. The relationship between matter (or energy) and curvature is given by

$$\varepsilon^{ab}[g_{\alpha\beta}, R^{\alpha}_{\beta rs}] = \kappa T^{ab}, \quad (1.115)$$

where, ε^{ab} is a tensor function of metric and the curvature tensor, κ is the constant of proportionality. We can derive Einstein field equations by using Eq.(1.86) as

$$R_{bd;e} + R_{be;d} + R^a_{bde;c} = 0. \quad (1.116)$$

Multiplying by g^{ad} , the above equation reduces to

$$R_{;e} + 2R^a_{e;a} = 0. \quad (1.117)$$

After simplification,

$$(R^{ab} - \frac{1}{2}g^{ab}R)_{;a} = 0. \quad (1.118)$$

For a four dimensional continuum, the linear, symmetric and divergence free function of the curvature is

$$\varepsilon^{ab} = R^{ab} - \frac{1}{2}Rg^{ab}, \quad (1.119)$$

where, ε^{ab} is called the Einstein tensor. Putting value of ε^{ab} in Eq.(1.115), we get

$$R^{ab} - \frac{1}{2}Rg^{ab} = \kappa T^{ab}. \quad (1.120)$$

The above equation is known as the Einstein field equations.

1.10 Cosmology

The term cosmology is derived from two Greek words, cosmos, “the Universe” and logos, “study”, therefore the scientific study of large scale properties of the Universe as a whole is called cosmology. It includes the origin, evolution and the ultimate fate of the Universe. From the beginning, it had been the fundamental quest of mankind to explore and understand the Universe and its matter content. The history of cosmology starts approximately 4000 years ago from the Babylonians who predicted the apparent motion of the Moon, stars, planets and the Sun in the sky. In the 4th century BC, the ancient Greeks built the first cosmological model which represents the motion of the Sun, the Moon and the planets around the spherical Earth every 24 hours. Further developments had been made regarding this model in the following centuries. In the 16th century, Nicolaus Copernicus proposed a heliocentric theory and constructed a model in which Earth, together with the other planets revolved in circular orbits around the Sun. In the same century, Tycho Brahe proposed that *if the Earth orbits the Sun, then the nearby stars should periodically change their positions as viewed from different parts of the Earth*. This shift in the position of the stars was known as the Stellar Parallax. Unfortunately, there was no practical evidence of this parallax. In the 17th century, when the first known telescope to be used as a scientific instrument had been invented by Galileo Galilei, he discovered moons orbiting the planet Jupiter, which revealed the fact that if moons could orbit another planet, why could not the planets orbit the Sun? In the same century, Tycho Brahe’s assistant, Johannes Kepler provided the foundation for our present conception of the Solar system with the laws that explained elliptical orbits

of the planets around the Sun. Later, Isaac Newton showed that the elliptical motion could be explained by his inverse-square law for the gravitational force. Within the 17th century, thousands of new stars were discovered and the cosmos seemed to be a vast sea of stars. In the 18th century, Immanuel Kant introduced the concept of Island Universes which refers to the location and description of nebulae. In 1785 William Herschel proposed the central position of our sun in the Milky Way. In the 19th century, the astronomer and mathematician Friedrich Bessel measured the distance of the Earth to the stars. The nearest star turned out to be about 25×10^6 million miles away.

The 20th century brought further insights in unlocking the mysteries of the Universe. GR played a significant role in the history of cosmology and the Einstein field equations given in this theory first predicted the expansion of the Universe. Later, in 1922, Alexander Friedmann gave the first solution of Einstein field equations predicting the expansion of the Universe which was confirmed by Edwin Hubble in 1929 by measuring the redshift of distant galaxies. He examined a linear relationship between the distance and redshift of galaxies which was later named as Hubble law. The various solutions of the Einstein Field Equations made the scientists and astronomers think that the Universe had been created at just one instant about some 10 Billion years ago and the galaxies were traveling away from us which creates expansion of the Universe. The British astronomer Fred Hoyle named that instant as Big Bang. In 1948, Herman Bondi, Thomas Gold and Fred Hoyle published some papers on the alternative theory of Big Bang known as the Steady state theory which explains that although the Universe is expanding, the matter content in it is continuously created to maintain the density of the Universe. This model also opposes the fact that the Universe has a beginning and an end. Steady state model had been rejected by many cosmologists, as the observational evidence favors for the Big Bang model. In 1949 Ralph Asher Alpher and Robert Hermann predicted the faint afterglow of the intense radiation of a hot Big Bang, which is later in 1965 confirmed by the discovery of Cosmic Microwave Background radiations (CMB). Since 1970 almost all cosmologists had accepted the Big Bang model and was still finding answers regarding the Universe.

Over decades, many cosmological models had been presented to evolved the humanity's understanding of the Universe but our main point of concern is with the Friedmann cosmological model.

1.10.1 The Friedmann Models of the Universe

In 1922, Alexander Friedmann who was famous for his ideas of expanding Universe gave a solution to Einstein field equations. His model describes the expansion as well as the geometry of the Universe within the context of GR. Two basic assumptions of this model are homogeneity and isotropy which are collectively known as the Cosmological principle [9]. Homogeneity means that the matter distribution in the Universe is same for all observers. Likewise, isotropy mean that the Universe appears same if it can be viewed from different directions. Friedmann model of Universe is given by the following metric.

$$ds^2 = c^2 dt^2 - a_k^2(t)[d\chi^2 + f_k^2(\chi)d\Omega^2], \quad (1.121)$$

where,

$$d\Omega^2 = d\theta^2 + \sin^2 \theta d\phi^2, \quad (1.122)$$

and $a_k(t)$ is the expansion factor which measures the rate of expansion of the Universe. It is convenient to convert the cosmic time into conformal time $t = t(\eta)$ such that

$$cdt = a_k(\eta)d\eta. \quad (1.123)$$

Here t is the original time variable. It gives directly the proper time elapsed since the start of the expansion. Integrating the above equation, we get

$$t = \frac{1}{c} \int a_k(\eta)d\eta. \quad (1.124)$$

The metric in terms of conformal time is given by

$$ds^2 = a_k^2(\eta)[d\eta^2 - d\chi^2 - f_k^2(\chi)(d\theta^2 + \sin^2 \theta d\phi^2)]. \quad (1.125)$$

Depending on the value of curvature parameter k and $f_k(\chi)$, there exist three possibilities.

1.10.2 Closed Friedmann Universe

In this case, Friedmann model starts from the Big Bang at $\eta = 0$, expands to its maximum size, then shrinks and collapse to a Big crunch at $\eta = 2\pi$. Big Crunch is a possible scenario for the ultimate fate of the Universe, in which metric expansion of space eventually reverses and the Universe recollapses, ultimately ending as a black hole singularity or causing a reformation of the

Universe starting with another Big Bang.

For $k = 1$,

$$f_1(\chi) = \sin \chi \quad ; \quad (0 \leq \chi \leq \pi).$$

Putting $f_1(\chi)$ into the metric given in Eq.(1.121), we get

$$ds^2 = a_1^2(\eta)[d\eta^2 - d\chi^2 - \sin^2 \chi(d\theta^2 + \sin^2 \theta d\phi^2)]. \quad (1.126)$$

Solving the above metric into Einstein field equations gives two independent Friedmann equations which represents the cycloid equations. Solution of these equations for the closed Universe is given by

$$a_1(\eta) = \frac{a_0}{2}(1 - \cos \eta) \quad ; \quad (0 \leq \eta \leq 2\pi), \quad (1.127)$$

$$t_1(\eta) = \frac{a_0}{2c}(\eta - \sin \eta) \quad ; \quad (0 \leq \eta \leq 2\pi). \quad (1.128)$$

For $k=1$, the geometry of spacetime corresponds to 3-sphere or S^3 .

1.10.3 Flat Friedmann Universe

In this case, Friedmann model starts from the Big Bang at $\eta = 0$ and represents an eternal Universe that expands forever without limit.

For $k = 0$,

$$f_0(\chi) = \chi \quad ; \quad (0 \leq \chi < \infty).$$

Putting $f_0(\chi)$ into the metric given in Eq.(1.121), we get

$$ds^2 = a_0^2(\eta)[d\eta^2 - d\chi^2 - \chi^2(d\theta^2 + \sin^2 \theta d\phi^2)]. \quad (1.129)$$

Solving the above metric into Einstein field equations, we get

$$a_0(\eta) = \frac{a_0}{2}\eta^2 \quad ; \quad (0 \leq \eta < \infty), \quad (1.130)$$

$$t_0(\eta) = \frac{a_0}{6c}\eta^3 \quad ; \quad (0 \leq \eta < \infty). \quad (1.131)$$

For $k = 0$, the spacetime geometry corresponds to 3-cone (Hyper cone). In this case, we have flat space, not flat spacetime.

1.10.4 Open Friedmann Universe

In the case of open Friedmann Universe, model starts from the Big bang at $\eta = 0$ and does not have an end as in the case of flat Universe.

For $k=-1$,

$$f_{-1}(\chi) = \sinh \chi \quad ; \quad (0 \leq \chi \leq \infty).$$

Putting $f_{-1}(\chi)$ into the metric (1.90), we get

$$ds^2 = a_{-1}^2(\eta)[d\eta^2 - d\chi^2 - \sinh^2 \chi(d\theta^2 + \sin^2 \theta d\phi^2)]. \quad (1.132)$$

Solving the above metric into the Einstein field equations, we get

$$a_{-1}(\eta) = \frac{a_0}{2}[\cosh \eta - 1] \quad ; \quad (0 \leq \eta < \infty), \quad (1.133)$$

$$t_{-1}(\eta) = \frac{a_0}{2c}[\sinh \eta - \eta] \quad ; \quad (0 \leq \eta < \infty). \quad (1.134)$$

For $k=-1$, the geometry of spacetime corresponds to 3-Hyperboloid or H^3 .

Chapter 2

Black Holes and Their Singularities

The existence of invisible objects which pull things in is a generic prediction of GR that attracted both the scientific world and general public. The possibility of the existence of such compact objects was first proposed by John Michell in a letter published in 1783. He named these objects “dark stars” [10]. In 1967, John Archibald Wheeler first used the term “black holes” for these dark stars during his lecture at the Princeton University and the name stuck. A black hole can be defined as a region of spacetime possessing such a strong gravitational field that matter, radiation and not even light can escape from its surface. In classical physics, a black hole is an object consisting of particles on its surface whose escape velocity is greater than or equal to the speed of light such that the light did not reflect back due to which it becomes invisible and because of gravitational attraction, everything falls into it.

$$v_o = \sqrt{\frac{2Gm}{r}},$$

where v_o is the escape velocity, m is the mass of that object, G is the gravitational constant and r is the radial distance from the center of mass of an object [8].

A black hole is formed when a massive star collapses onto itself under the force of gravity. A nuclear fusion reaction occurring inside the core of the star provides it with sufficient energy to overcome the gravitational pressure. The fusion process burns hydrogen into helium which is converted into carbon, eventually ending up with the formation of iron. Lacking fuel for

further fusion, the gravitational pressure overcomes the internal pressure of a star due to which it collapses onto itself blowing the surface out under a massive supernova explosion producing shock waves in the fabric of spacetime. A star collapses completely into an infinite energy density called the singularity where the curvature of spacetime becomes infinite, the laws of physics, including GR, fail and even spacetime itself become meaningless. Another important feature of a black hole which covers the singularity is a surface at which the escape velocity is greater than or equal to the speed of light. This surface is known as an “event horizon” of a black hole and it can be defined as a null hypersurface which acts as a boundary between two regions of the spacetime, the exterior and interior of a black hole, clothing the singularity [11]. Any event that happened inside an event horizon do not affect the outside observer. On the basis of mass distribution, black holes can be characterized as

Stellar black holes	$\sim 10^{1/2} \text{ to } 10^2 M_{\odot}$
Intermediate black holes	$\sim 10^3 \text{ to } 10^5 M_{\odot}$
Supermassive black holes	$\sim 10^6 \text{ to } 10^9 M_{\odot}$

where M_{\odot} is taken as the mass of the Sun. Stellar black holes are usually dense and smaller in size. There are an enormous number of stellar black holes in the Universe. These black holes consume the dust and gas around them and grow in size. The proper evidence of Intermediate black hole is not provided yet, but in 2014, it had been observed that a black hole is found in the arm of the spiral galaxy which appeared to be an Intermediate black hole. The most mysterious black holes found in the Universe are Supermassive black holes. They are often called “the monsters of the Universe”. They are very huge in size and formed when hundreds and thousands of Stellar and Intermediate black holes merge together. They are located at the center of each galaxy due to their enormous size and are growing day by day. A Supermassive black hole “Sagittarius A” is present at the center of our galaxy. Beside them, there is another kind of black hole which is not discovered yet, but they are considered to be formed after the Big Bang about 13.7 billion years ago. They are very small in size and known as “Primordial or miniature” black holes.

2.1 The Schwarzschild Black Hole

The Schwarzschild black hole is a static, spherically symmetric black hole of mass M with zero charge and angular momentum. The Einstein field equations (1.89) are highly non-linear second order PDE's which are too complicated to solve directly, therefore some assumptions had been made about spacetime symmetries of the solution. In 1916, Karl Schwarzschild presented a vacuum solution to Einstein field equations which described the gravitational field outside a spherical mass. The most general spherically symmetric and static metric in spherical polar coordinates (t, r, θ, ϕ) is given by

$$ds^2 = e^{v(t,r)} dt^2 - e^{\lambda(t,r)} dr^2 - R^2(t,r) d\Omega^2, \quad (2.1)$$

where v , λ and R are functions of time t and radial r coordinates, where

$$d\Omega^2 = d\theta^2 + \sin^2\theta d\phi^2. \quad (2.2)$$

Since spacetime is considered to be static, the gravitational field for a point mass does not vary with time, therefore the above metric reduces to

$$ds^2 = e^{v(r)} dt^2 - e^{\lambda(r)} dr^2 - R^2(r) d\Omega^2. \quad (2.3)$$

Without the loss of generality, $R^2(r)$ is taken as r^2 instead of a constant function, therefore the metric given in Eq.(2.3) becomes

$$ds^2 = e^{v(r)} dt^2 - e^{\lambda(r)} dr^2 - r^2 d\Omega^2. \quad (2.4)$$

The metric tensor and its inverse is given by

$$g_{ab} = \begin{bmatrix} e^{v(r)} & 0 & 0 & 0 \\ 0 & -e^{\lambda(r)} & 0 & 0 \\ 0 & 0 & -r^2 & 0 \\ 0 & 0 & 0 & -r^2 \sin^2\theta \end{bmatrix}, \quad (2.5)$$

$$g^{ab} = \begin{bmatrix} e^{-v(r)} & 0 & 0 & 0 \\ 0 & -e^{-\lambda(r)} & 0 & 0 \\ 0 & 0 & -\frac{1}{r^2} & 0 \\ 0 & 0 & 0 & -\frac{1}{r^2 \sin^2\theta} \end{bmatrix}. \quad (2.6)$$

The non-zero Christoffel symbols are

$$\begin{aligned}\Gamma_{0\ 1}^0 &= \frac{1}{2}v', & \Gamma_{0\ 0}^1 &= \frac{1}{2}v'e^{v-\lambda}, & \Gamma_{1\ 1}^1 &= \frac{1}{2\lambda'}, \\ \Gamma_{2\ 2}^1 &= -re^{-\lambda}, & \Gamma_{3\ 3}^1 &= -r\sin^2\theta e^{-\lambda}, & \Gamma_{1\ 2}^2 &= \frac{1}{r} = \Gamma_{1\ 3}^3, \\ \Gamma_{3\ 3}^2 &= -\sin\theta\cos\theta, & \Gamma_{2\ 3}^3 &= \cot\theta.\end{aligned}\tag{2.7}$$

For vacuum solution, the Einstein field equations reduces to

$$R_{ab} = 0.\tag{2.8}$$

The surviving components are

$$R_{oo} = v'' + \frac{1}{2v'}(v' - \lambda' + \frac{2v'}{r}) = 0,\tag{2.9}$$

$$R_{11} = -v'' - \frac{1}{2v'}(v' - \lambda' - \frac{2\lambda'}{r}) = 0,\tag{2.10}$$

$$R_{22} = 1 - e^{-\lambda} + \frac{1}{2r}(\lambda' - v')e^{-\lambda} = 0,\tag{2.11}$$

$$R_{33} = R_{22}\sin^2\theta = 0.\tag{2.12}$$

Adding Eq.(2.9) and (2.10), we get

$$\frac{2v'}{r} + \frac{2\lambda'}{r} = 0,\tag{2.13}$$

$$v' + \lambda' = 0.\tag{2.14}$$

Integrating the above equation yields

$$v + \lambda = \text{constant}.\tag{2.15}$$

Absorbing the constant in to the units of measurement of time, we have

$$v(r) = -\lambda(r).\tag{2.16}$$

Putting value of $v(r)$ in Eq.(2.11)

$$(-re^{-\lambda})' + 1 = 0.\tag{2.17}$$

Integrating the above equation and dividing by r , we get

$$e^{v(r)} = 1 + \frac{\alpha}{r}, \quad (2.18)$$

since, $v = -\lambda$, so we have

$$e^{-\lambda(r)} = 1 + \frac{\alpha}{r}, \quad (2.19)$$

where, $\alpha = -\frac{2Gm}{c^2}$ [8]. Therefore Eq.(2.18) and (2.19) becomes

$$e^{v(r)} = 1 - \frac{2Gm}{c^2 r}, \quad (2.20)$$

$$e^{-\lambda(r)} = 1 - \frac{2Gm}{c^2 r}. \quad (2.21)$$

Putting the value of $e^{v(r)}$ and $e^{-\lambda}$ in Eq.(2.4), we get

$$ds^2 = c^2 \left(1 - \frac{2Gm}{c^2 r}\right) dt^2 - \left(1 - \frac{2Gm}{c^2 r}\right)^{-1} dr^2 - r^2 d\Omega^2. \quad (2.22)$$

The boundary $r_s = \frac{2Gm}{c^2}$ is called an event horizon of the Schwarzschild black hole. As $r \rightarrow \infty$, the metric reduces to Minkowski spacetime.

2.1.1 Singularities of the Schwarzschild Black Hole

There are two type of singularities in the Schwarzschild metric which can be determined by the following curvature invariants

$$R_1 = 0, \quad (2.23)$$

$$R_2 = \frac{48G^2 m^2}{c^4 r^6}, \quad (2.24)$$

$$R_3 = \frac{64G^3 m^3}{c^6 r^6}. \quad (2.25)$$

Clearly, the singularity located at $r = 0$ is essential while coordinate singularity appears at $r = r_s$. Since the metric is singular at $r = r_s$, it does not give any physical information for $r < r_s$.

2.1.2 Eddington-Finkelstein Coordinates

The Schwarzschild coordinates fail to give information about any physical feature present at and beyond the event horizon $r = r_s$, therefore a new set of coordinates must be required for $r \leq r_s$. Arthur Eddington [12] constructed a new coordinate system which was then rediscovered by David Finkelstein [13]. These null coordinates are given by

$$v = \frac{1}{\sqrt{2}}(ct + r), \quad (2.26)$$

$$u = \frac{1}{\sqrt{2}}(ct - r), \quad (2.27)$$

where v and u are called advanced and retarded time. To remove singularity at $r = r_s$, they had defined a new radial coordinate as

$$r^* = \int \frac{dr}{1 - 2Gm/c^2r}, \quad (2.28)$$

$$r^* = r + r_s \ln \left| \frac{r}{r_s} - 1 \right|, \quad (2.29)$$

the constant of integration is taken to make the argument of the logarithm dimensionless. Redefining the advanced and retarded time in terms of r^* , we get

$$dv = \frac{1}{\sqrt{2}} \left(cdt + \frac{dr}{1 - r_s/r} \right), \quad (2.30)$$

$$du = \frac{1}{\sqrt{2}} \left(cdt - \frac{dr}{1 - r_s/r} \right). \quad (2.31)$$

The Schwarzschild metric in terms of advanced and retarded coordinates is given by

$$ds^2 = 2(1 - r_s/r)dv^2 - 2\sqrt{2}dvdr - r^2d\Omega^2, \quad (2.32)$$

$$ds^2 = 2(1 - r_s/r)du^2 + 2\sqrt{2}dudr - r^2d\Omega^2. \quad (2.33)$$

Putting $r = r_s$ in Eq.(2.32) and Eq.(2.33), we get $g_{00} = 0$. Moreover the value of determinant g is finite, therefore the singularity at $r = r_s$ has been removed by using advanced and retarded time coordinates. These coordinates are known as Eddington-Finkelstein coordinates. The metrics given in Eq.(2.32) is purely in terms of advance time while the metric given in Eq.(2.33) is in terms of retarded time. Both the metrics are independent of each other. The

singularity is removed by using these coordinates, however, if we want to solve a metric for both the advanced and retarded coordinates, we can use them simultaneously. Adding Eq.(2.30) and Eq.(2.31), we get

$$dt = \frac{1}{\sqrt{2}c}(dv + du). \quad (2.34)$$

Subtracting Eq.(2.30) and Eq.(2.31), we get

$$\frac{dr}{1 - r_s/r} = \frac{1}{\sqrt{2}}(dv - du). \quad (2.35)$$

Taking square of Eq.(2.34) and Eq.(2.35) and substituting the value in Eq.(2.22), we get

$$ds^2 = 2(1 - r_s/r)dudv - r^2d\Omega^2. \quad (2.36)$$

Eddington-Finkelstein coordinates are good enough to study at $r \geq r_s$ but not consistent for $r < r_s$, therefore a more convenient coordinates must be required to study the properties of Schwarzschild black hole beyond that point.

2.1.3 Kruskal Coordinates

To describe the properties of the Schwarzschild black hole at $r = r_s$, Martin Kruskal exponentiated the Eddington-Finkelstein coordinates and two new constants α and β were introduced to cover the entire manifold of the maximally extended Schwarzschild solution by a single patch of coordinates [8]. The Kruskal coordinates are defined as

$$V = \alpha e^{v/\beta}, \quad (2.37)$$

$$U = -\alpha e^{-u/\beta}. \quad (2.38)$$

Multiplying Eq.(2.37) and Eq.(2.38), we get

$$VU = -\alpha^2 e^{(v-u)/\beta}, \quad (2.39)$$

The above equation can be rewritten in terms of new radial coordinate r^* as

$$VU = -\alpha^2 e^{\sqrt{2}r^*/\beta}. \quad (2.40)$$

Using Eq.(2.29), we get

$$VU = -\alpha^2 \left| \frac{r}{r_s} - 1 \right|^{\sqrt{2}r_s/\beta}. \quad (2.41)$$

Taking differentials of Eq.(2.37) and Eq.(2.38) and multiplying the results, we get

$$dudv = 2\left(\frac{r_s}{\alpha}\right)^2 \left(\frac{r}{r_s} - 1\right)^{-1} e^{-r/r_s} dU dV. \quad (2.42)$$

Inserting this value in Eq.(2.36), we get

$$ds^2 = \frac{4r_s^2}{\alpha^2 r} e^{-r/r_s} dU dV - r^2 d\Omega^2. \quad (2.43)$$

Putting $r = r_s$ in the above metric requires no singularity as $g \neq 0$. Normally α is chosen to be unity, but for U, V to have units of length, α can be taken as $2r_s$ in which case $g_{01} = r_s = g_{10}$.

2.1.4 Kruskal-Szekeres Coordinates

A convenient coordinate system which can be obtained from the Kruskal coordinates are called the Kruskal-Szekeres coordinates. It has a time-like T and a space-like coordinate R defined as,

$$T = \frac{1}{\sqrt{2}}(V - U), \quad (2.44)$$

$$R = \frac{1}{\sqrt{2}}(V + U), \quad (2.45)$$

with $\alpha = 1$, taking the differentials of Eq.(2.44) and Eq.(2.45), we get

$$dT = \frac{1}{\sqrt{2}}(dV - dU), \quad (2.46)$$

$$dR = \frac{1}{\sqrt{2}}(dV + dU). \quad (2.47)$$

Adding and subtracting Eq.(2.46) and Eq.(2.47)

$$dV = \frac{1}{\sqrt{2}}(dT + dR), \quad (2.48)$$

$$dU = -\frac{1}{\sqrt{2}}(dT - dR). \quad (2.49)$$

Multiplying Eq.(2.48) and Eq.(2.49), we get

$$dV dU = -\frac{1}{2}(dT^2 - dR^2). \quad (2.50)$$

Inserting this value in the metric given in Eq.(2.43), we get

$$ds^2 = 2\frac{r_s}{r}e^{-r/r_s}(dT^2 - dR^2) - r^2d\Omega^2, \quad (2.51)$$

where,

$$R^2 - T^2 = 2(r/r_s)e^{r/r_s},$$

and

$$T/R = \tan(t/2r_s). \quad (2.52)$$

Here T varies from $-\infty$ to ∞ and R from 0 to ∞ .

2.1.5 The Compactified Kruskal-Szekeres Coordinates

Kruskal coordinates (V, U) and Kruskal-Szekeres coordinates (T, R) can be compactified to obtain a new set of coordinate having finite range of values. This new set of coordinate is called the compactified Kruskal-Szekeres coordinates. The transformation of Kruskal coordinates into the compactified Kruskal coordinates is given by

$$M = \tan^{-1} V, \quad (2.53)$$

$$N = \tan^{-1} U, \quad (2.54)$$

where the ranges $(-\infty, \infty)$ mapped on to $(-\frac{\pi}{2}, \frac{\pi}{2})$. Using Eq.(2.53) and Eq.(2.54) in Eq.(2.51)

$$ds^2 = \frac{4r_s^3 e^{-r/r_s}}{r \cos^2 M \cos^2 N} dM dN - r^2 d\Omega^2. \quad (2.55)$$

Now clearly, the above metric is singular at $r = 0$, while $(M, N) = (-\frac{\pi}{2}, \frac{\pi}{2})$ at $r = r_s$. The Kruskal-Szekeres coordinates can be compactified by using the following transformations

$$\Phi = \tan^{-1}(T + R) + \tan^{-1}(T - R), \quad (2.56)$$

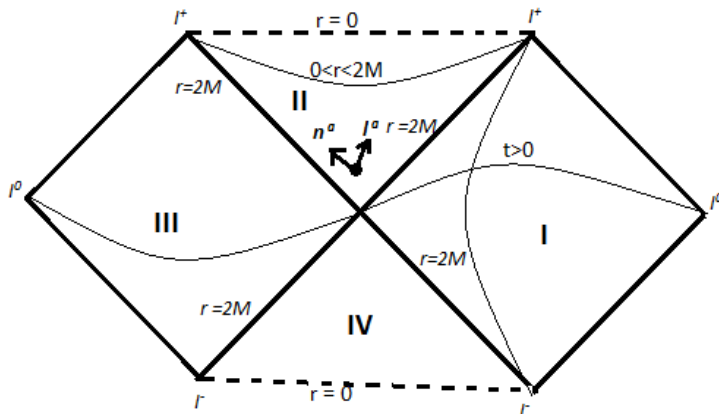


Figure 2.1: The Carter-Penrose diagram for maximally extended Schwarzschild solution.

$$\Psi = \tan^{-1}(T + R) + \tan^{-1}(T - R). \quad (2.57)$$

Figure 2.1 represents the Schwarzschild spacetime in compactified Kruskal-Szekeres coordinates. This diagram is known as the Carter-Penrose diagram, developed by Brandon Carter and Roger Penrose so that spacetime structure can be visualized in a two dimensional plane.

2.2 Reissner-Nördstrom Black Hole

Reissner-Nördstrom (RN) black hole is a static, spherically symmetric black hole of mass M possessing an electric charge Q with zero angular momentum [11]. Hans Reissner and Gunnar Nördstrom gave a gravitational solution to the Einstein-Maxwell field equations. We will start with the same spherically symmetric and static metric along with the Christoffel symbols and Ricci scalars given in Eq.(2.7), Eq.(2.9) and Eq.(2.10). The difference arises due to the presence of a charge Q which involves electromagnetism. The electromagnetic four-vector potential for source-free Maxwell equations coupled with gravity is given by

$$A_a = (Q/cr, 0).$$

Now the Maxwell tensor, which gives the electromagnetic field is

$$F = d \wedge A,$$

which implies

$$F_{ab} = -F_{ba} = 2 \delta_{[a}^0 \delta_{b]}^1 Q / cr^2. \quad (2.58)$$

The stress-energy tensor for the electric field is given by

$$T^{ab} = \frac{1}{4\pi} (F^{ac} F_c^b - \frac{1}{4} g^{ab} F^{cd} F_{cd}). \quad (2.59)$$

Putting this value in Eq.(2.58), stress-energy tensor in mixed form is given by

$$\begin{aligned} T_0^0 = T_1^1 = -T_2^2 = -T_3^3 &= Q^2 e^{-(\nu+\lambda)/8\pi c^2 r^4}, \\ T_b^a &= 0 \quad ; \quad a \neq b. \end{aligned} \quad (2.60)$$

Since the solution is assumed to be static and spherically symmetric so $T_{ab} = 0$ and $T_0^0 = T_1^1$. Using Eq.(2.9) and Eq.(2.10), we get

$$\nu'(r) + \lambda'(r) = 0, \quad (2.61)$$

Integrating the above equation, we get

$$\nu(r) + \lambda(r) = 0, \quad (2.62)$$

where, $R_{22} = \kappa T_2^2$. Using Eq.(2.11), we get

$$-\frac{1}{r^2} [(-r e^{-\lambda})' + 1] = -\frac{8\pi G}{c^2} \frac{Q^2}{8\pi c^2 r^4}. \quad (2.63)$$

Solving the above equation, we get

$$e^{\nu(r)} = e^{-\lambda(r)} = 1 + \frac{\alpha}{r} + \frac{GQ^2}{c^4 r^2}, \quad (2.64)$$

where,

$$\alpha = -\frac{2Gm}{c^2}.$$

Putting value of $e^{\nu(r)}$, $e^{-\lambda(r)}$ and α in the metric given in Eq.(2.4), we get

$$ds^2 = \left(1 - \frac{2Gm}{c^2 r} + \frac{GQ^2}{c^4 r^2}\right) c^2 dt^2 - \left(1 - \frac{2Gm}{c^2 r} + \frac{GQ^2}{c^4 r^2}\right)^{-1} dr^2 - r^2 d\Omega^2. \quad (2.65)$$

The above metric is known as RN metric. If we put $Q = 0$ in the above metric, it will lead to the Schwarzschild exterior solution. Also consider the case when $Q = 0$ and $Q^2 = Gm^2$. If $Q = 0$, RN metric reduces to Schwarzschild metric as $r_s = r_+ + r_-$ so the outer horizon r_+ becomes the Schwarzschild event horizon whereas inner horizon (r_-) collapses to essential singularity. If $Q^2 = Gm^2$, then according to Eq.(2.69) and Eq.(2.70) we are left with $r_s = 2r_+ = 2r_-$. The solution in this case is called the Extreme RN solution.

2.3 Kerr Black Hole

In 1963, a New Zealand mathematician Roy Patrick Kerr discovered a solution to the Einstein field equations that describes the gravitational field of a rotating, uncharged and axially symmetric body of mass M with angular momentum J . The standard Kerr metric in Boyer-Lindquist coordinates is given by

$$ds^2 = \left(1 - \frac{2Gmr}{c^2\rho^2}\right)c^2 dt^2 - \left(\frac{\rho^2}{\Delta}\right)dr^2 - \rho^2 d\theta^2 - \left[\left(r^2 + \frac{a^2}{c^2}\right)\sin^2\theta + \frac{2Gmra^2}{\rho^2 c^2} \sin^4\theta\right]d\phi^2 + \left(\frac{2Gmra \sin^2\theta}{\rho^2 c^2}\right)dt d\phi, \quad (2.66)$$

where,

$$\rho^2 = r^2 + \frac{a^2 \cos^2\theta}{c^2}, \quad (2.67)$$

$$\Delta = r^2 - \frac{2Gmr}{c^2} + \frac{a^2}{c^2}. \quad (2.68)$$

Due to the spin angular momentum of a gravitational source, the inertial frames are dragged along with the rotation. Like the Schwarzschild and RN metric, they are also solution of the vacuum Einstein field equations.

2.4 Kerr-Newmann Black Hole

Kerr Newmann black hole is the generalization of RN black hole, also known as the charged Kerr black holes as it describes the gravitational field of a

rotating, axisymmetric, charged body of mass M with angular momentum J . Kerr-Newmann metric is given as

$$\begin{aligned}
 ds^2 = & \left[1 - \frac{\left(\frac{2Gmr}{c^2} - \frac{GQ^2}{c^4}\right)}{\rho^2}\right]c^2 dt^2 - \left(\frac{\rho^2}{\Delta}\right)dr^2 - \rho^2 d\theta^2 - \left[\left(r^2 + \frac{a^2}{c^2}\right) \sin^2 \theta \right. \\
 & \left. + \frac{2Gmra^2 \sin^2 \theta}{\rho^2 c^4}\right]d\phi^2 + \left(\frac{2Gmra \sin^2 \theta}{\rho c^2}\right)dt d\phi, \quad (2.69)
 \end{aligned}$$

where,

$$\rho^2 = r^2 + a^2 \frac{\cos^2 \theta}{c^2}, \quad (2.70)$$

$$\Delta = r^2 - \frac{2Gmr}{c^2} + \frac{G\theta^2}{c^4} + \frac{a^2}{c^2}. \quad (2.71)$$

Now consider, if we put $a = 0$ in the above metric it reduces to RN metric. Similarly, putting $Q = 0$ the metric reduces to Kerr solution. In Kerr metric given in Eq.(2.97) if we put $a = 0$ it yields Schwarzschild metric.

Chapter 3

The Suture Model

In the first chapter, a brief discussion about the closed Friedmann Universe had been provided. In this chapter, I will review the Suture Model for the case of a closed Friedmann Universe including its boundary conditions and the evaluation of mass of a black hole, observed from the boundary between the interior Friedmann and exterior Schwarzschild regions. To understand the dynamics of Suture Model, it is necessary to define some terms first, which are given below.

Mean Extrinsic Curvature

In the context of GR, the curvature of spacetime is expressed by the Einstein tensor in the Einstein field equations. In order to understand the implications of Einstein field equations on the hypersurface, R_{bcd}^a must be decomposed into its spatial parts. This decomposition can be done by a tensor, which measures the intrinsic curvature of the hypersurface. The intrinsic curvature tensor does not provide any information about the hypersurface, therefore a purely spatial and symmetric curvature tensor is defined for the hypersurfaces, known as the extrinsic curvature tensor. It is defined as the projection of the spacetime covariant derivative of the normal to the hypersurface. The extrinsic curvature tensor measures how a normal vector to the hypersurface changes from one point to another. But, in any case

$$K^a_b = n^a_{;b}. \quad (3.1)$$

The mean extrinsic curvature measures the fractional change in the 3 dimen-

sional volume along the normal n^a , defined by the following formula:

$$K = -\nabla \cdot \mathbf{n}, \quad (3.2)$$

Foliation of Spacetime

In the context of GR, foliation is the splitting of a 4-dimensional spacetime back into 3-dimensional space and 1-dimensional time. In other words, foliation is a procedure by which spacetime can be expressed as a series of spatial slices which evolves in time. The purpose of foliating a spacetime is to study its dynamics and to understand its geometry more precisely. A spacetime can be foliated by hypersurfaces which are characterized as time-like, light-like and space-like depending on the value of line element

$$ds^2 = g_{ab}dx^a dx^b. \quad (3.3)$$

For all dx^a lying in the hypersurface,
 if $g_{ab}dx^a dx^b > 0$, then it is time-like;
 if $g_{ab}dx^a dx^b = 0$, then it is light-like;
 if $g_{ab}dx^a dx^b < 0$, then it is space-like.

Maximal Slicing

A hypersurface for which mean extrinsic curvature tensor is zero everywhere is called a maximal hypersurface. It encloses maximum volume for a particular given area. If the foliation is done by the maximal hypersurfaces, then this type of foliation is called maximal foliation or maximal slicing. Therefore, Eq.(3.2) can be used for maximal foliation as $K = 0$.

York-Time

If the spacetime is foliated by a sequence of space-like hypersurfaces whose mean extrinsic curvature is constant, then it is called K -slicing or York slicing. In this case, each spacetime event lies on a unique space-like hypersurface at a specific value of time. A time parameter is provided to hypersurfaces such that its value varies from one slice to another but constant at each slice throughout. This time parameter is known as the York time .

Penrose's Conjecture

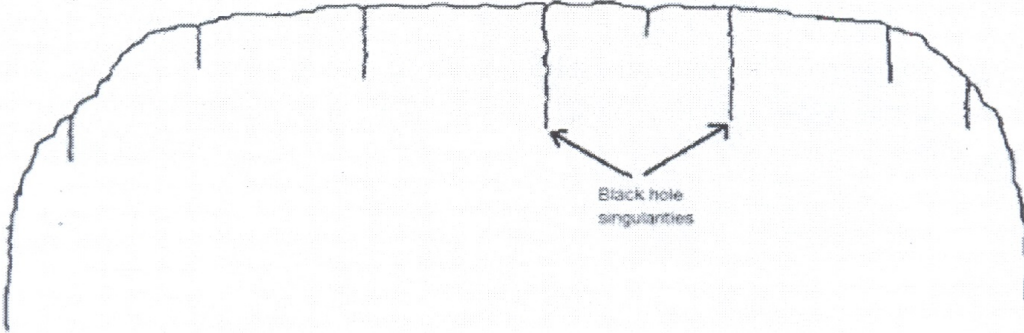


Figure 3.1: Penrose picture showing the roof of a cave as the final singularity while the stalactites as the black hole singularities [15].

Penrose conjectured that in a closed Universe, it may be possible to regard the black hole singularity as a part of the final cosmological singularity while for an open Universe, as a part of compactification of spacetime. Penrose explained this conjecture by considering an example of a cave whose roof consisted of a large number of stalactites, the roof corresponds to the final singularity while the stalactites to the black hole singularities as shown in Figure 3.1. He argued that by some conformal transformation, it should be possible to straighten out the roof and have it appear smooth, i.e, there should exist a foliation of spacetime by a sequence of space-like hypersurfaces which would approach the singularity smoothly without cutting it anywhere, thus the entire spacetime would be foliated.

In order to investigate the conjecture of Penrose, various inhomogeneous cosmological models had been proposed. The Schwarzschild lattice Universe and the Suture Model are the two most consistent and concise models of closed Universe presented by Qadir and Wheeler. The former is described in the following section while the latter shows the formation of a black hole due to the evolution of two closed Friedmann Universes. The behavior in the last stages of crunch (the final singularity) had been investigated by foliating these models by the sequence of space-like hypersurfaces of constant mean extrinsic curvature.

3.1 The Schwarzschild Lattice Universe

Schwarzschild lattice Universe was the simplest model which was constructed to study the dynamics of the closed Universe and its behavior at the final singularity. First attempt to make a closed Universe was made by considering polytopes with the number of faces 4, 6, 8 or 12. The possible combination for tetrahedra could be made by using 5, 16 or 600 faces but it gave the worse approximation to the topology of a sphere, therefore a better approximation was made by considering the cubes, octahedra and dodecahedra. The inaccuracy was further improved by taking 120 cells of identical masses and enclosed them in a regular lattice which possesses the topology of a 3-sphere as shown in Figure 3.2. To obtain the appearance of a Friedmann Universe, they had joined these cells in such a way that each cell contained pure empty-space Schwarzschild geometry, hence we can say that many Schwarzschild zones were fitted together to make a closed Universe [16]. This was a Schwarzschild lattice Universe model, in which the cells possess the features of Schwarzschild geometry while the space between cells follows a Friedmann evolution. The interface between the two lattice cell is specified by the motion of test particle falling towards the Schwarzschild singularity. This fact can be explained by considering the behavior of a test particle at the interface between two of the Schwarzschild black holes. Due to the gravitational forces of Schwarzschild black holes, the test particle first rises at the same time and then falls back which makes the two centers oscillate. In this way, the lattice Universe expands and contracts which arose the features of Friedmann Universe in it although, it does not involve the Friedmann geometry [16]. As my point of concern is the Suture Model, therefore I am not going into the mathematics of the Schwarzschild lattice Universe but will give a brief review on foliation of it.

3.1.1 Foliation of Schwarzschild Lattice Universe

This model was K -foliated by a sequence of space-like hypersurfaces by treating each cell independently as a Schwarzschild geometry and requiring that the mean extrinsic curvature of the foliating hypersurfaces have zero derivatives on the boundary B . For the solution to be unique, conditions were provided at the boundary and center of the cell [16]. Since the singularity of a black hole is located at the center and the space-like hypersurface is non-singular everywhere, so the treatment had to be made at the center.

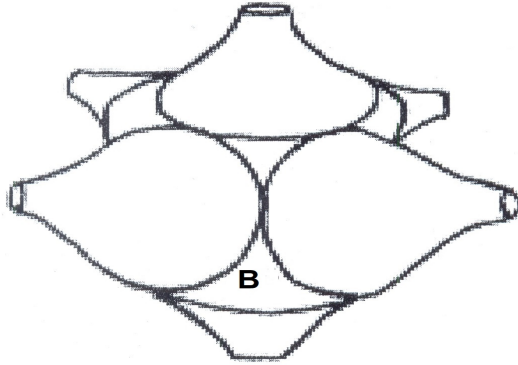


Figure 3.2: The Schwarzschild lattice Universe [16].

However, by requiring that the extrinsic curvature and hence the York time becomes infinite at the singularity, no hypersurface of finite mean extrinsic curvature would hit the singularity. This foliation covers the initial singularity like many one-finger gloves applied one over the other to a finger such that no glove except the last one would touch the finger. This fact is illustrated in Figure 3.3. This implies that none of the sequences of space-like hypersurfaces touches the singularity but their limit coincides with the Schwarzschild singularity located at $r = 0$. Since the foliation runs smoothly with no problem anywhere, thus Brill, Cavallo and Isenberg [19] noticed that the K -slicing is more appropriate foliation procedure than the maximal slicing.

3.1.2 Modification of Schwarzschild Lattice Universe

If we fit this model in accordance with the picture of a cave presented by Penrose, it comes out that there would be no stalactites on the roof of the cave. More precisely, the problem was that the black holes were already present in the lattice cell, they did not formed during the evolution of the whole model. The purpose was to construct a model in which a black hole should be formed and observed during the evolution of the model. This problem was solved when one of the lattice cells was replaced by a thin shell of dust in such a way that its exterior geometry was Schwarzschild while the interior one was that of Minkowski [17]. The distribution of mass inside the

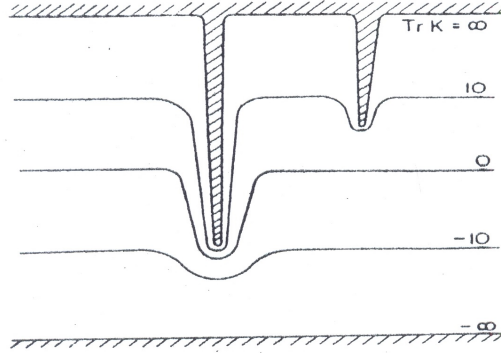


Figure 3.3: Schematic picture of the gloving of a black hole singularity by a sequence of space-like hypersurfaces of increasing mean extrinsic curvature [16].

shell itself can be compared to the sprinkling of stars in the plane of a galaxy [18]. The geometry of such a thin shell of dust in an asymptotically flat spacetime had been studied by Israel [19]. This replacement did not disturb the rest of the lattice Universe. A suitable boundary condition was used to connect the Minkowski geometry with the Schwarzschild outside the shell. The same foliation procedure was followed in this case and again proceeded without facing any problem. However, this model still lacked physical clarity as the black holes were not formed, they were already present in the model. Moreover, the basic drawback in the models mentioned above was that if we extrapolate backward in time, they were unable to provide any information about the beginning of the Universe, so there was a need to construct a model which should be consistent with the whole geometry of a 3-sphere and would be able to collapse in to the Big Bang. For this purpose, Qadir and Wheeler constructed a Suture Model which contained a clear message about the final stages of crunch. The dynamics and a brief description about this model is given in the following section.

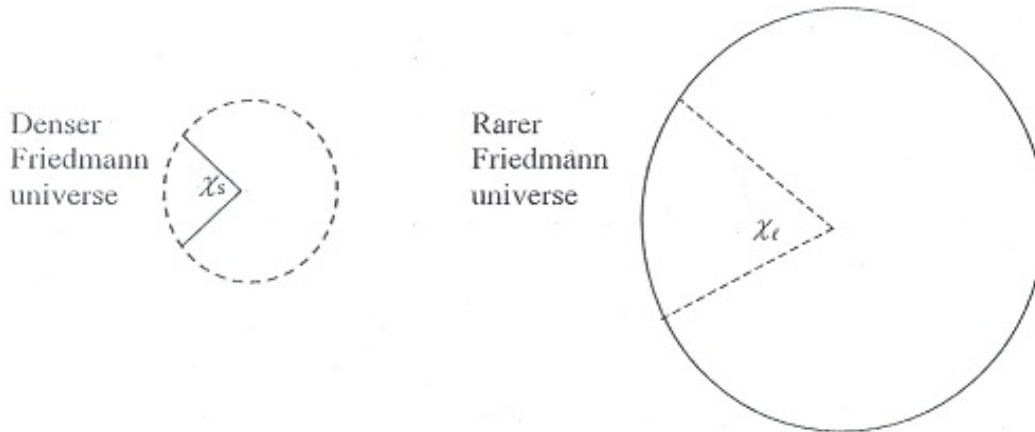


Figure 3.4: The cut and paste view of the Suture Model with two dimensions suppressed. The denser Friedmann Universe contains the hyperspherical angle χ_s as the radial parameter, whereas χ_l is the hyperspherical angle for the rarer Universe [20].

3.2 The Suture Model

The Suture Model was constructed by the well-understood geometries of two closed Friedmann Universes and Schwarzschild spacetime which I had explained in chapters 1 and 2. Since the Friedmann Universe is homogeneous, a cut and paste method was used to introduce the inhomogeneity. Two purely matter filled Friedmann Universes of different densities at the phase of their maximum expansion were considered. The denser Friedmann Universe was labeled as region A, the rarer one as B and the Schwarzschild region as region C. A section of $1/N$ of its volume had been cut out from the rarer Universe and replaced by the section of denser one in such a way that the mass of the model remains unchanged as shown in Figure 3.4. These two regions were then joined together by the Schwarzschild geometry provided that, if we extrapolate backward in time, all the three regions merge together and no cracks or gaps should appear in the limit at their junction. Since the Schwarzschild geometry sandwiched between the two Friedmann Universes, it is also known as the Sandwich Model. The cut and paste view of Suture Model is given in Figure 3.5.

3.2.1 Features of Suture Model

This model could be distinguished from the lattice Universe in a sense that it was required to possess the following features:

1. This model must contain matter distribution;
2. During the whole expansion of the Friedmann Universe, a black hole must be formed;
3. There must be an apparent asymmetry between the Big Bang and Big Crunch;
4. There should be a smooth evolution of a black hole and the Universe from Big Bang to Big Crunch.

Since the densities of the two Friedmann Universes are not the same, the denser Universe expands, goes to its maximum expansion and begin to contract while the rarer one is still expanding, due to which the crunch appears earlier in the denser region. Therefore the denser region collapses at a faster rate than the rarer region. As a result, a black hole is created in the denser region and can be seen by an observer in the rarer region. Meanwhile the rarer region is still expanding. This well defined model is known as the Suture Model. The dynamics of this model had been investigated by foliating it with the space-like hypersurfaces of constant mean extrinsic curvature. The entire 3-geometry ultimately collapses in to a space-like singularity.

3.2.2 Parameters of Suture Model

The space-like hypersurfaces are spherically symmetric and independent of the angles θ and ϕ . Therefore, the Friedmann region can be purely described in terms of two parameters, i.e the Friedmann time parameter η and the hyperspherical angle χ . Similarly, the Schwarzschild region is described in terms of its radial r and time t parameters in the usual Schwarzschild coordinates. From the point of view of an observer located in the denser Friedmann region whose geometry is given by the following metric, the evolution proceed normally.

$$ds^2 = a^2(\eta)[d\eta^2 - d\chi_s^2 - \sin^2 \chi_s(d\theta^2 + \sin^2 \theta d\phi^2)], \quad (3.4)$$

where,

$$a(\eta) = \frac{a_{0s}}{2}(1 - \cos \eta), \quad (3.5)$$

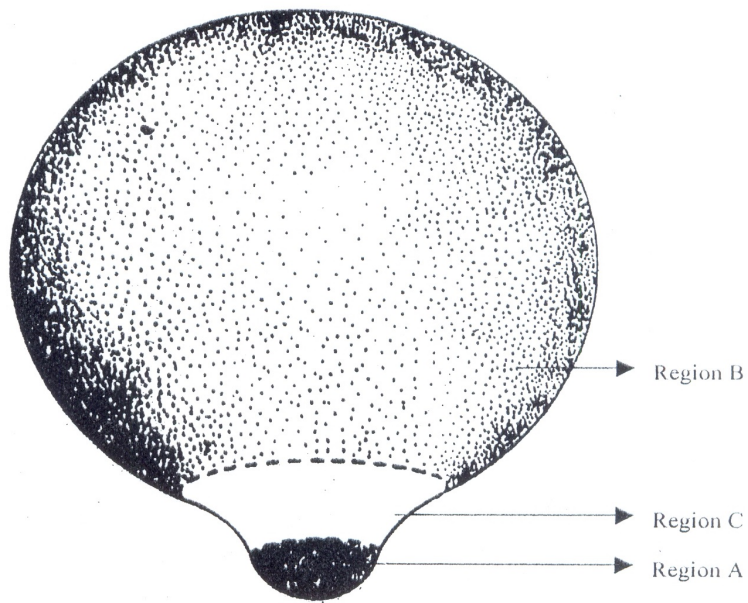


Figure 3.5: The cut and paste view of the Suture Model with two dimension suppressed [20].

η , being the time parameter for the denser Friedmann region going from 0 at the Big Bang, through π at the phase of maximum expansion, to 2π at the Big Crunch, where a_{0_s} is the radius of the denser Friedmann Universe at the phase of maximum expansion. The radial parameter χ_s , goes from 0 at the center of the region to some χ_M at the junction with the Schwarzschild region. For the section of denser Friedmann region to remain unchanged, χ_s has to be constant over the entire evolution of the model. Similarly, for an observer in the rarer Friedmann region given by the following metric, the evolution proceeds normally

$$ds^2 = a^2(\eta)[d\eta^2 - d\chi_l^2 - \sin^2 \chi_l(d\theta^2 + \sin^2 \theta d\phi^2)], \quad (3.6)$$

where,

$$a(\eta) = \frac{a_{0_l}}{2}(1 - \cos \eta), \quad (3.7)$$

η and χ_l are the time and radial parameters and a_{0_l} is the radius of the rarer Friedmann Universe at the phase of maximum expansion. The radial parameter χ_l goes from χ_p to π as shown in the Figure 3.6.

3.2.3 Boundary Conditions of Suture Model

The solution measured purely in terms of time parameter, η and the hyper-spherical angle, χ , is homogeneous and isotropic everywhere in the interior of the Friedmann region but this condition breaks at the boundary which lies at some radius $\chi = \chi_s$. Therefore, suitable matching conditions should be defined so that the interior Friedmann geometry must match smoothly on to exterior Schwarzschild geometry. The boundary conditions for the three regions are given below

Boundary Between Region A and C

The circumference relation at the boundary between Friedmann region and the Schwarzschild region is given by

$$C_s = 2\pi R_s, \quad (3.8)$$

where, R_s is the r value of the Schwarzschild region at the boundary between the regions A and C. By comparing Eq.(2.22) and Eq.(3.4), the expansion factor (a) is related to R_s as

$$R_s = a \sin \chi_s. \quad (3.9)$$

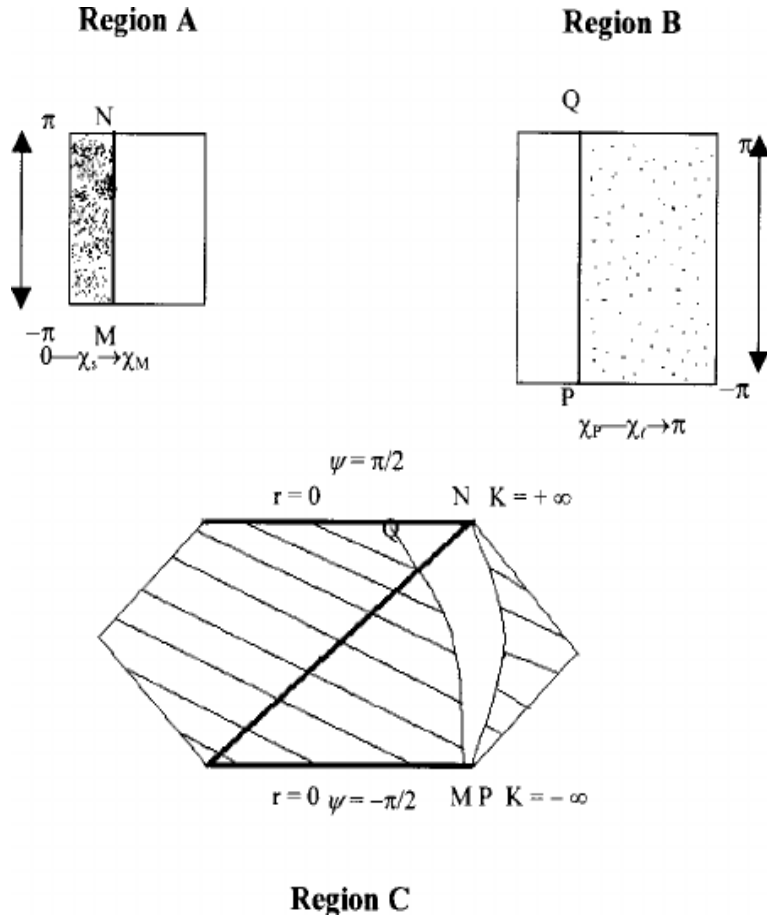


Figure 3.6: The CP diagram for the Suture Model. For region A, the time parameter η goes from 0 to 2π , while χ_s varies from 0 to χ_M . In region B, variation of η is same while χ_l varies from χ_p to π . In region C, the time parameter Φ goes from $-\pi/2$ to $\pi/2$ corresponding to the initial singularity to the final singularity at $r = 0$. The York time K goes from $-\infty$ to ∞ for these singularities [20].

Substituting this value in Eq.(3.8), we get

$$C_s = 2\pi a \sin \chi_s. \quad (3.10)$$

Using Eq.(3.5), we get

$$C_s = \pi[a_{0_s} \sin \chi_s(1 - \cos \eta)]. \quad (3.11)$$

Boundary Between Region B and C

At the boundary between region B and C, the similar equation holds with R_l as the r value of Schwarzschild region, i.e

$$C_l = 2\pi R_l, \quad (3.12)$$

where, the expansion factor (a) is related to R_l as

$$R_l = a \sin \chi_l. \quad (3.13)$$

Substituting Eq.(3.7) in the above equation, we get

$$C_l = \pi[a_{0_l} \sin \chi_l(1 - \cos \eta)]. \quad (3.14)$$

Generally, the match is possible for the boundaries between all the three region for all values of η , if

$$R_k = a \sin \chi_k, \quad (3.15)$$

where,

$$a = \frac{a_{0_k}}{2}(1 - \cos \eta). \quad (3.16)$$

Putting this value in Eq.(3.15), we get

$$R_k = \frac{a_{0_k}}{2} \sin \chi_k(1 - \cos \eta). \quad (3.17)$$

Therefore, in general

$$C_k = 2\pi R_k, \quad (3.18)$$

$$C_k = \pi[a_{0_k} \sin \chi_k(1 - \cos \eta)]. \quad (3.19)$$

Comparing Eq.(3.18) and Eq.(3.19), we get

$$R_k = \frac{a_{0_k}}{2} \sin \chi_k(1 - \cos \eta), \quad (3.20)$$

$$1 - \cos \eta = \frac{2R_k}{a_{0_k} \sin \chi_k}. \quad (3.21)$$

3.2.4 Calculation of the Mass Discrepancy of Suture Model

As discussed earlier, due to the difference of densities of the two Friedmann Universes, the rate of their evolution is different, as a result, the denser Friedmann Universe collapses to a black hole and can be viewed by an observer at the boundary of region B and C. At the phase of maximum expansion, the density of region A is taken to be 4 times the density of region B. By integrating this density, the mass of both the regions can be calculated, but due to the curvature of Friedmann geometry, there would be some difference between the mass obtained by integrating the density and the mass as a gravitational source of denser Friedmann region. The boundary conditions can be used to calculate the mass of a black hole observed from the boundary between the region B and C. Consider a purely spatial metric for a sphere and space-like section of Schwarzschild section embedded in a Euclidean space, where w is the embedding parameter, i.e. $r = r(w)$ and $w = w(\sigma)$. The metric is given by

$$ds^2 = d\sigma^2 + R^2(\sigma)[d\theta^2 + \sin^2\theta d\phi^2]. \quad (3.22)$$

The relation between σ and w is given by the following equation

$$dw^2 = d\sigma^2 - dR^2, \quad (3.23)$$

Comparing the above metric with the space-like section of Friedmann metric, we get

$$d\sigma^2 = a^2 d\chi^2 \quad ; \quad R^2 = a^2 \sin^2\chi d\chi^2. \quad (3.24)$$

Substituting values of $d\sigma$ and dR in Eq.(3.23), we get

$$dw = a \sin\chi d\chi. \quad (3.25)$$

Slope of simultaneity associated with the world line of a particle in Friedmann geometry is given by

$$\frac{dw}{dR} = \frac{R}{\sqrt{a^2 - R^2}}. \quad (3.26)$$

Similarly, comparing the metric given in Eq.(3.22) with the space-like section of the Schwarzschild metric, we get

$$d\sigma^2 = \frac{dR^2}{1 - \frac{2Gm}{c^2 R}}. \quad (3.27)$$

Substituting value of $d\sigma$ in Eq.(3.23), we get

$$dw = \frac{dR}{\sqrt{\frac{c^2 R}{2Gm} - 1}}. \quad (3.28)$$

Slope of simultaneity associated with the world line of a particle in Schwarzschild geometry is given by

$$\frac{dw}{dR} = \frac{1}{\sqrt{\frac{c^2 R}{2Gm} - 1}}. \quad (3.29)$$

Comparing Eq.(3.26) and Eq.(3.28), we get

$$\frac{a^2}{R^2} = \frac{c^2 R}{2Gm}. \quad (3.30)$$

Therefore, in general the mass of a denser Friedmann region which collapses in to a black hole as observed from the boundary between region B and C is given by

$$m = \frac{c^2}{2G} a \sin^3 \chi_l. \quad (3.31)$$

The mass as seen from the surface of a black hole can be find out by integrating the density of Friedmann region over volume of a black hole. The density of Friedmann region at the phase of maximum expansion is given by

$$\rho_s = \frac{3}{8\pi a^2}. \quad (3.32)$$

Integrating this density over the volume, we get

$$m_s = \frac{3}{4} (\chi_s - \frac{1}{2} \sin 2\chi_s) a. \quad (3.33)$$

Substituting the value of a from Eq.(3.31), we get

$$m_s = \frac{3G}{2c^2} (\chi_s - \frac{1}{2} \sin 2\chi_s) \csc^3 \chi_l m. \quad (3.34)$$

Now, from Eq.(3.31) and Eq.(3.34), it is clear that $m_s \neq m$. Thus there is a difference of mass as seen from the surface of black hole and the mass as seen from the boundary of rarer Friedmann and Schwarzschild region, i.e.

$$\frac{\delta m}{m} = \frac{m - m_s}{m}. \quad (3.35)$$

Substituting values of m and m_s , we get

$$\frac{\delta m}{m} = 1 - \frac{3G}{2c^2} (\chi_s - \frac{1}{2} \sin 2\chi_s) \csc^3 \chi_l. \quad (3.36)$$

3.2.5 Foliation of Suture Model

After defining the boundary conditions for the Suture Model, it was K -foliated with the guess value of η chosen at $\chi = 0$ in region A. After foliating this model, it was observed that the size of the Universe varies with the value of K as shown in the Figure 3.7. The diagram starts with the York time at $-\infty$, where both the closed Friedmann Universes completely merges in to each other showing the time of Big Bang at $\eta = 0$. After that, they started expanding and the Schwarzschild region starts appearing. As, the denser Friedmann region contracts, the rarer one will first expands but by the time the black hole had formed, the rarer Friedmann region started its collapse. With the passage of York time, the distance between the regions increases while the volume starts shrinking, both regions more or less disappears while the Schwarzschild region only contributes and it seems as a corridor between two regions. This result is discussed in detail in the conclusion.

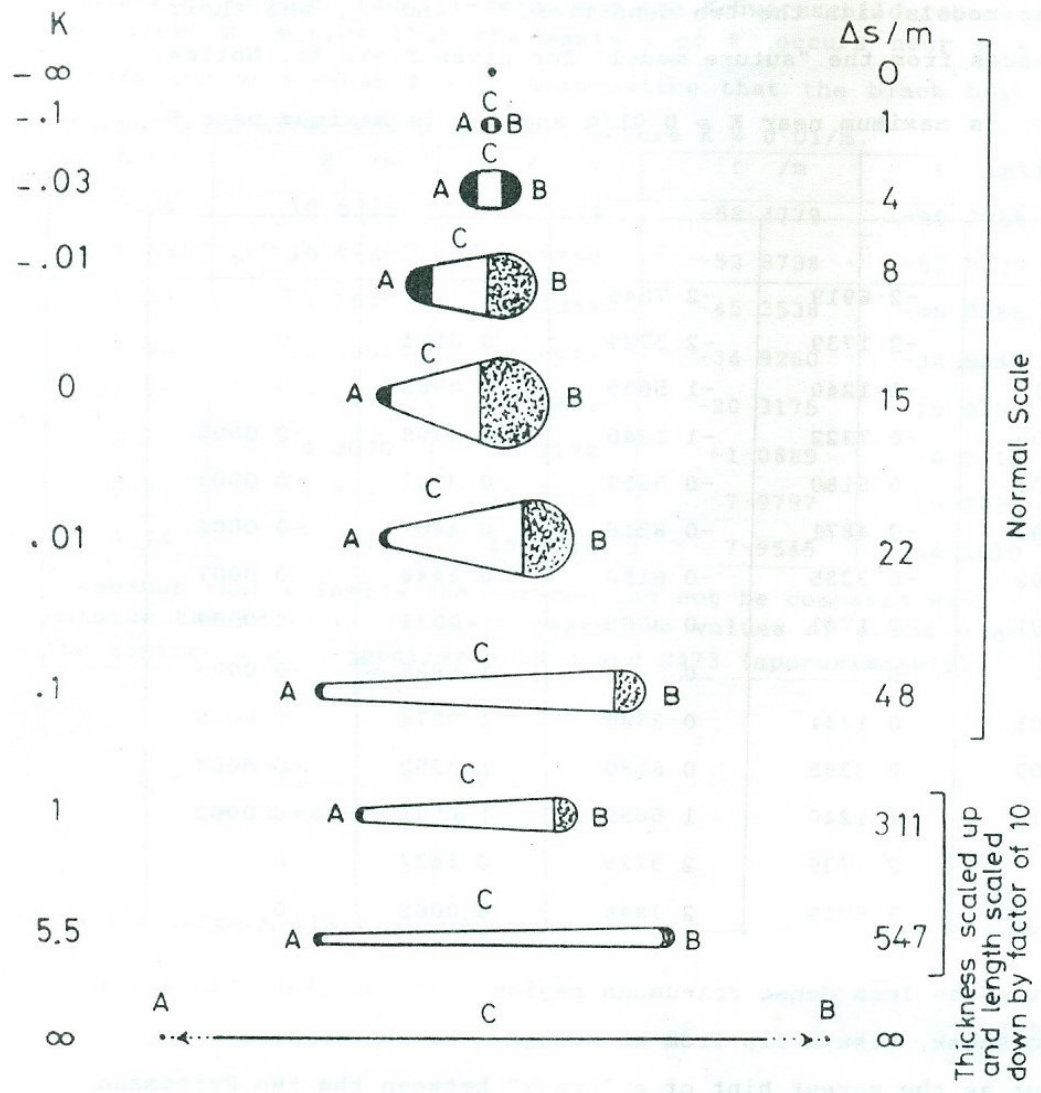


Figure 3.7: The variation of the size of Universe during the evolution of Suture Model from Big Bang to Big Crunch [17].

Chapter 4

The Extended Suture Models

In the previous chapter, the dynamics of the Suture Model was explained where two closed Friedman Universes were considered and during the course of their evolution, the behavior of the model was studied. Now, considering the Universe to be open or flat, the Suture Model can be extended to the two cases:

- (1) Open Suture Model
- (2) Flat Suture Model

Since, the flat and the open Friedmann Universe have no final singularity (section 1.11.3 and 1.11.4), i.e. their time-like (η) and the angle-like (χ) parameters are infinite. Therefore, to construct a model in general for both the cases, they must be limited to some finite value. For this purpose, I have defined the transformations which compactify these infinite Universes separately. In topological terms, compactification is a method of converting an infinite topological space into a compact space. A compact space is generally a closed and bounded space. The Universes under consideration are non-compact or infinite, therefore it is not possible to study the formation of a black hole during their evolution. In order to study the dynamics of a non-compact Universe, we first need to convert it into a compact or finite space. This could be done by transforming the coordinates in which the Universe is defined. The new finite coordinates are called compactified coordinates which mapped the infinity to a finite value.

4.1 Open Suture Model

The open Suture Model is constructed by considering a denser closed Friedmann Universe and a rarer compactified open Friedmann Universe of the same volume. A section of $1/N$ of the volume of denser Friedmann Universe is cut out and replaced by the rarer compactified open Friedmann Universe such that the mass of the model remains the same as shown in Figure 4.1. Both the regions are then joined together by the Schwarzschild geometry. The open Suture Model follows the same requirements and the geometry as the Suture Model (section 3.2.1) except for the region B which corresponds to the 3-Hyperboloid structure for an open Friedmann Universe. The cut and paste view of open Suture Model is given in Figure 4.2. Since, η and χ go to infinity, therefore I have defined new parameters η' and χ' as the inverse tangent function of η and χ which mapped them to a finite value $\frac{\pi}{2}$. The transformations are defined as

$$\chi' = \tan^{-1} \chi, \quad 0 \leq \chi \leq \infty \quad (4.1)$$

$$\eta' = \tan^{-1} \eta, \quad 0 \leq \eta \leq \infty \quad (4.2)$$

where, $0 \leq \chi' \leq \frac{\pi}{2}$; $0 \leq \eta' \leq \frac{\pi}{2}$. The Friedmann metric in compactified coordinates becomes

$$ds^2 = a^2(\eta')[\sec^2 \eta' d\eta'^2 - \sec^2 \chi'_s d\chi'_s{}^2 - \sinh^2(\tan \chi'_s) d\Omega^2], \quad (4.3)$$

where,

$$d\Omega^2 = d\theta^2 + \sin^2 \theta d\phi^2. \quad (4.4)$$

The expansion factor and the cosmic time in terms of compactified coordinates is given by

$$a(\eta') = \frac{a_0}{2}[\cosh(\tan \eta') - 1], \quad (4.5)$$

$$t(\eta') = \frac{a_0}{2}[\sinh(\tan \eta') - \tan \eta']. \quad (4.6)$$

At $\eta' = 0$, $a(\eta') = 0$ and $t(\eta') = 0$ while at $\eta' = \frac{\pi}{2}$, $a(\eta')$ and $t(\eta')$ becomes infinite. From the point of view of an observer located in the closed Friedmann region, the evolution would proceed normally in the open Friedmann region. The metric for the closed Friedmann region is given by

$$ds^2 = a^2(\eta)[d\eta^2 - d\chi_{s'}^2 - \sin^2 \chi_{s'}(d\theta^2 + \sin^2 \theta d\phi^2)], \quad (4.7)$$

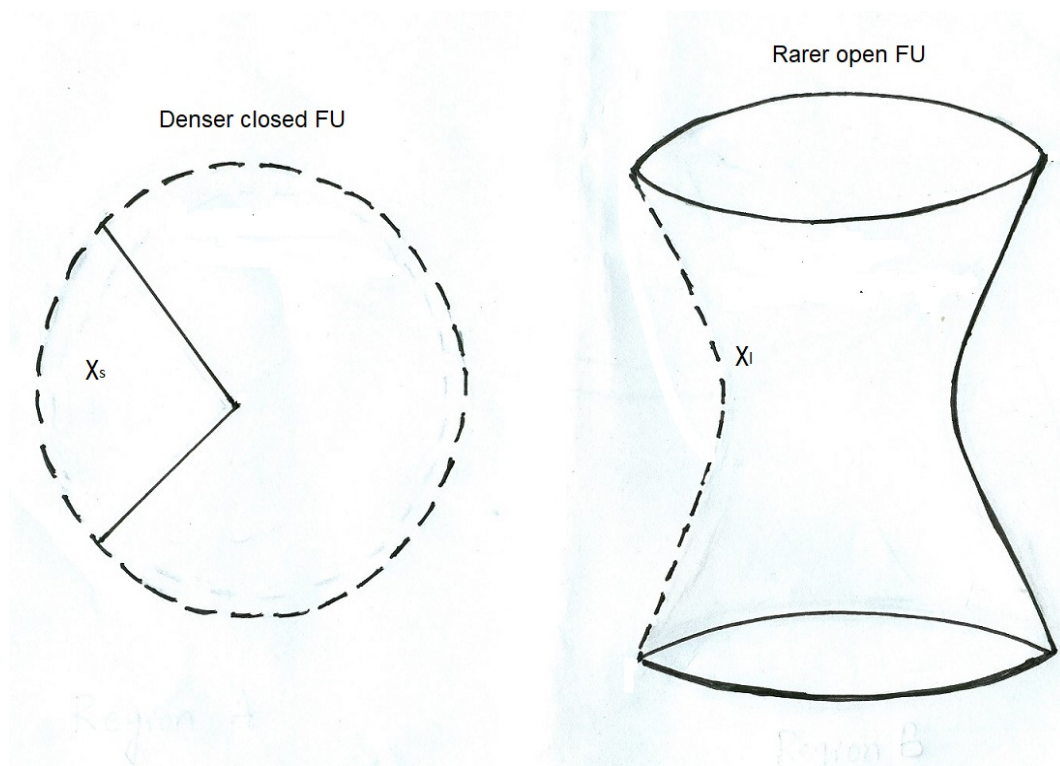


Figure 4.1: The cut and paste view of the open Suture Model with two dimensions suppressed. The denser closed Friedmann Universe contains the hyperspherical angle $\chi_{s'}$, as the radial parameter, whereas $\chi_{l'}$, is the hyperspherical angle for the rarer open Friedmann Universe.

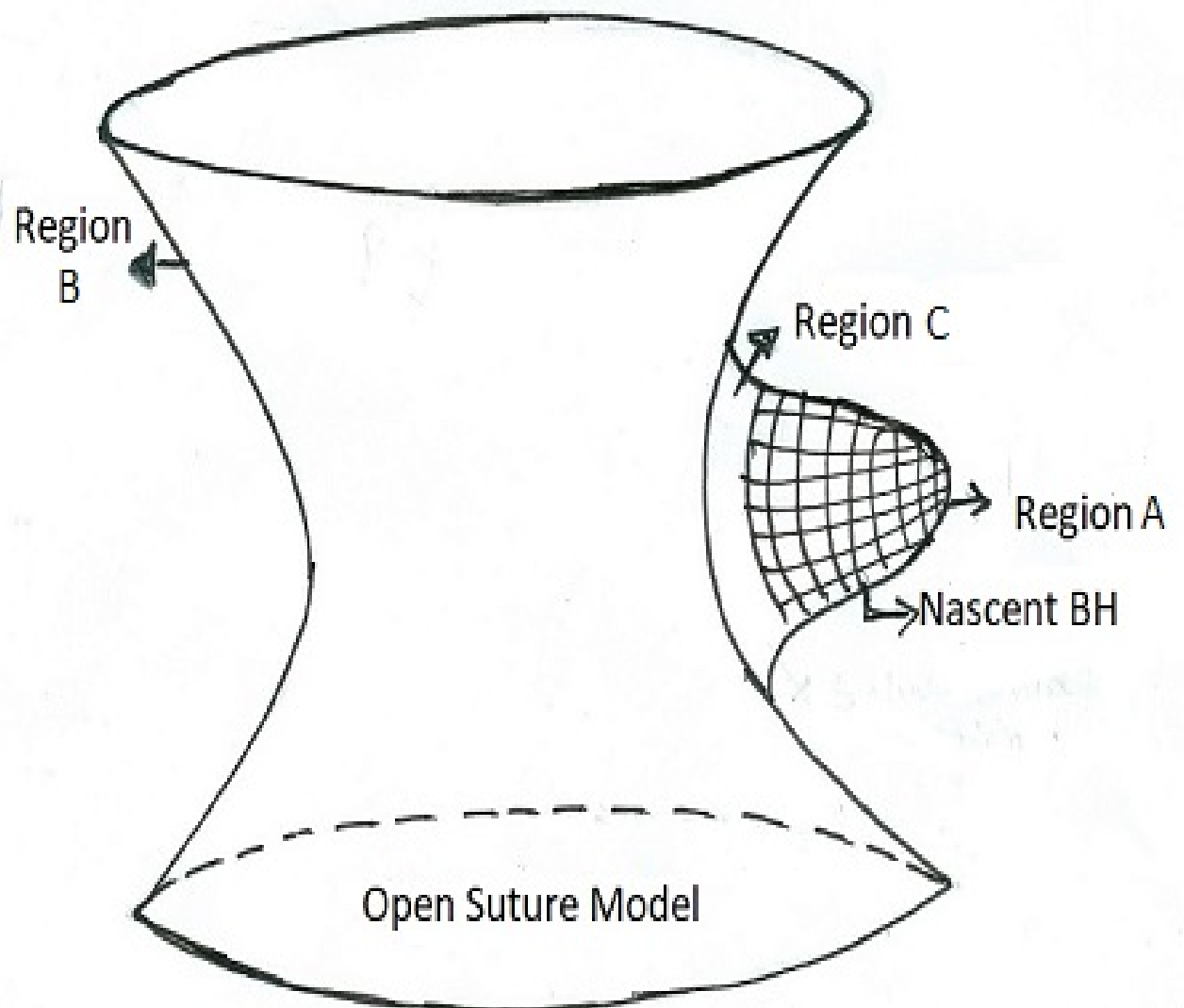


Figure 4.2: The cut and paste view of the open Suture Model with two dimension suppressed.

where, the variations of parameters would be same as mentioned in the section (3.2.2). The metric for an open Friedmann region in compactified coordinates is given by

$$ds^2 = a^2(\eta')[\sec^2 \eta' d\eta'^2 - \sec^2 \chi'_l d\chi'^2_l - \sinh^2(\tan \chi'_l) d\Omega^2]. \quad (4.8)$$

where,

$$d\Omega^2 = d\theta^2 + \sin^2 \theta d\phi^2. \quad (4.9)$$

The radial parameter $\chi_{s'}$ goes from 0 at the center of region A to some $\chi_{M'}$ at the junction with the Schwarzschild region. For region A, $\chi_{s'}$ has to be constant over the entire evolution. The parameter for region B varies from some χ'_l to $\frac{\pi}{2}$ as shown in the Figure 4.3.

4.1.1 Boundary Conditions for the Open Suture Model

The solution measured in terms of compactified coordinates, η' and the hyperspherical angle, χ' , is homogeneous and isotropic everywhere in the interior of both of the Friedmann regions but this condition breaks at the boundary, which lies at some radius $\chi' = \chi'_{s'}$. Therefore, suitable matching conditions should be defined so that the interior Friedmann geometry must match smoothly on to the exterior Schwarzschild geometry.

Boundary Between Region A and C

The circumference relation at the boundary between Friedmann region and the Schwarzschild region is given by

$$C_{s'} = 2\pi R_{s'}, \quad (4.10)$$

where, $R_{s'}$ is the r value of the Schwarzschild region at the boundary between the regions A and C. The expansion factor (a) is related to $R_{s'}$ as

$$R_{s'} = a \sin \chi_{s'}. \quad (4.11)$$

Substituting this value in Eq.(4.10), we get

$$C_{s'} = 2\pi a \sin \chi_{s'}. \quad (4.12)$$

Using Eq.(3.7) for denser Friedmann region, we get

$$C_{s'} = \pi [a_{0s'} \sin \chi_{s'} (1 - \cos \eta)]. \quad (4.13)$$

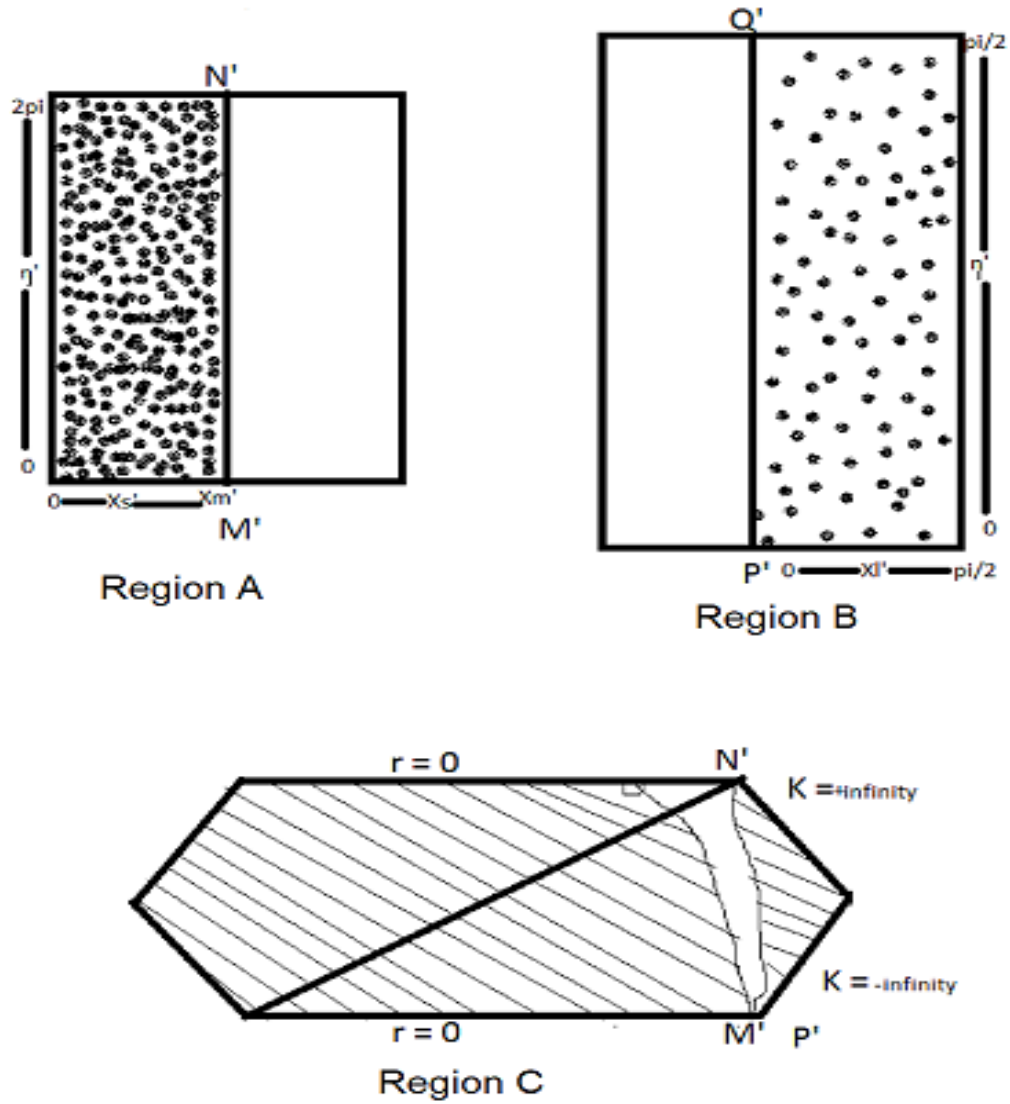


Figure 4.3: The CP diagram for the open Suture Model. For region A, the time parameter η goes from 0 to 2π , while χ_s varies from 0 to χ_M . In region B, η' varies from 0 to $\frac{\pi}{2}$ while χ_l varies from $\chi_{p'}$ to $\frac{\pi}{2}$. In region C, the time parameter Φ goes from $-\pi/2$ to $\pi/2$ corresponding to the initial singularity to the final singularity at $r = 0$. The York time K goes from $-\infty$ to ∞ for these singularities [20].

Boundary Between Region B and C

The relation between the circumference and the radius of the Schwarzschild region at the boundary between open Friedmann Universe and the Schwarzschild region is given by

$$C_{l'} = 2\pi R_{l'}, \quad (4.14)$$

where, $R_{l'}$ is the r value of the Schwarzschild region at the boundary between region B and C and the expansion factor (a) is related to $R_{l'}$ as

$$R_{l'} = a(\eta') \sinh(\tan \chi_{l'}). \quad ; \quad 0 \leq \chi_{l'} \leq \frac{\pi}{2} \quad (4.15)$$

Substituting Eq.(4.5) in Eq.(4.15), we get

$$R_{l'} = \frac{a_{0l'}}{2} [\cosh(\tan \eta') - 1] \sinh(\tan \chi_{l'}). \quad (4.16)$$

Therefore, Eq.(4.14) becomes

$$C_{l'} = a_{0l'} \pi [(\cosh(\tan \eta') - 1) \sinh(\tan \chi_{l'})]. \quad (4.17)$$

4.1.2 Calculation of the Mass Discrepancy of the Open Suture Model

As discussed in section (3.2.4), in the case of Suture Model, the density of region A was taken to be 4 times the density of region B at the phase of maximum expansion. Since both the Friedmann regions were closed, therefore they had same variations of η and χ . Now, for the open Suture Model, as the variations of η and χ for both the Friedmann regions are not same, therefore for definiteness, the density of the closed denser region is taken to be 4 times the density of the compactified open rarer region at the phase of their maximum expansion. Since, in this case, the phase of maximum expansion of both the Friedmann regions are not same, therefore their density ratio is arbitrarily chosen for a definite value. Similar to the previous work, there are two types of masses to be work out, one by integrating the density and the other by using the boundary conditions. Comparing the metric given in Eq.(3.22) with the space-like section of open Friedmann metric in compactified coordinates, we get

$$d\sigma^2 = a^2(\eta') \sec^2 \chi' d\chi'^2 \quad ; \quad R^2(\eta') = a^2(\eta') \sin^2 h(\tan \chi'). \quad (4.18)$$

Substituting the value of $d\sigma$ and dR in Eq.(3.22), we get

$$dw = -a(\eta') \sec \chi' d\chi' \sinh(\tan \chi'). \quad (4.19)$$

Slope of simultaneity associated with the world line of a particle in Friedmann compactified geometry is given by

$$\frac{dw}{dR} = -\frac{1}{\sqrt{\frac{a^2(\eta')}{R^2(\eta')} + 1}}. \quad (4.20)$$

Comparing Eq.(3.29) and Eq.(4.20), we get

$$\frac{a^2(\eta')}{R^2} = \frac{c^2 R}{2Gm}. \quad (4.21)$$

Therefore, the mass of a black hole as observed from the boundary between region B and C in an open Suture Model is given by

$$m = \frac{a(\eta')c^2}{2G} \sinh^3(\tan \chi'). \quad (4.22)$$

The mass as seen from the surface of a black hole is calculated in the section (3.2.4). It would be the same except for the notation, I have used for the denser closed Friedmann region, i.e.

$$m_{s'} = \frac{3}{4}(\chi_{s'} - \frac{1}{2} \sin 2\chi_{s'})a(\eta). \quad (4.23)$$

The mass expression obtained in Eq.(4.22) is in compactified coordinate while the mass expression in Eq.(4.23) is in terms of the original coordinates. In terms of the original time and angle coordinates, Eq.(4.31) becomes

$$m = \frac{a(\eta)c^2}{2G} [\cosh \eta - 1] \sinh^3 \chi'. \quad (4.24)$$

Now, it is clear from the above equation that the mass as seen from the boundary of open Friedmann region and the Schwarzschild region is dependent on η and χ which are the function of η' and χ' respectively, as given in Eq.(4.1) and Eq.(4.2). At $\eta' = 0$, the value of η becomes zero according to the transformation defined in Eq.(4.1). Putting $\eta = \eta' = 0$ in Eq.(4.23) and Eq.(4.24) implies the time of Big Bang where all the three regions merges

together to a single point. Similarly, at $\chi' = 0$, the value of χ becomes zero according to the Eq.(4.2). Putting $\chi = \chi' = 0$ in Eq.(4.23) and Eq.(4.24), we get $m_{s'} = m = 0$. The difference between both the masses is significant when I match the upper limits of η and χ . At $\eta' = \frac{\pi}{2}$, the value of η becomes infinite. Putting this value in Eq.(4.24), the mass seen from the boundary between open Friedmann and the Schwarzschild region would be infinite. Same will be the case with $\chi' = \frac{\pi}{2}$. So, there is a clear difference of the mass as seen from the surface and the mass as seen from the boundary of region A and C in case of the open Suture Model. To find the mass discrepancy, for definiteness, I have chosen $\eta = \frac{\pi}{2}$ for both the Friedmann regions. The expansion factor for the region A would be $\frac{a_0}{2}$ at $\eta = \frac{\pi}{2}$. Therefore Eq.(4.23) becomes

$$m_{s'} = \frac{3}{4}(\chi_{s'} - \frac{1}{2} \sin 2\chi_{s'}) \frac{a_0}{2}. \quad (4.25)$$

The expansion factor in terms of original coordinates for the region B at $\eta = \frac{\pi}{2}$ is given by

$$a(\eta) = \frac{a_0}{2}(6.1020 \times 10^{38}). \quad (4.26)$$

Substituting Eq.(4.26) in Eq.(4.24) and rearranging, we get

$$\frac{a_0}{2} = (3.28 \times 10^{-39}) \frac{Gm}{c^2} \csc h^3 \chi_{\nu}. \quad (4.27)$$

Substituting Eq.(4.27) in Eq.(4.25), we get

$$m_{s'} = (3.28 \times 10^{-39}) \frac{3G}{4c^2} [\chi_{s'} - \frac{1}{2} \sin 2\chi_{s'}] \csc h^3 \chi_{\nu} m. \quad (4.28)$$

Thus, the mass discrepancy for an open Suture Model is given by

$$\frac{\delta m}{m} = 1 - [(3.28 \times 10^{-39}) \frac{3G}{4c^2} (\chi_{s'} - \frac{1}{2} \sin 2\chi_{s'}) \csc h^3 \chi_{\nu}]. \quad (4.29)$$

The open Suture Model can be foliated by the sequence of space-like hypersurfaces of constant mean extrinsic curvature. This work is not yet done, however, we can assume the possibility that the open Suture Model will behave likewise the Suture Model, i.e, the distance between the two regions increases to infinity as the York time proceeds while the volume shrinks to zero. The rough sketch of the expected behavior of the model during the whole evolution is given in Fig 4.4.

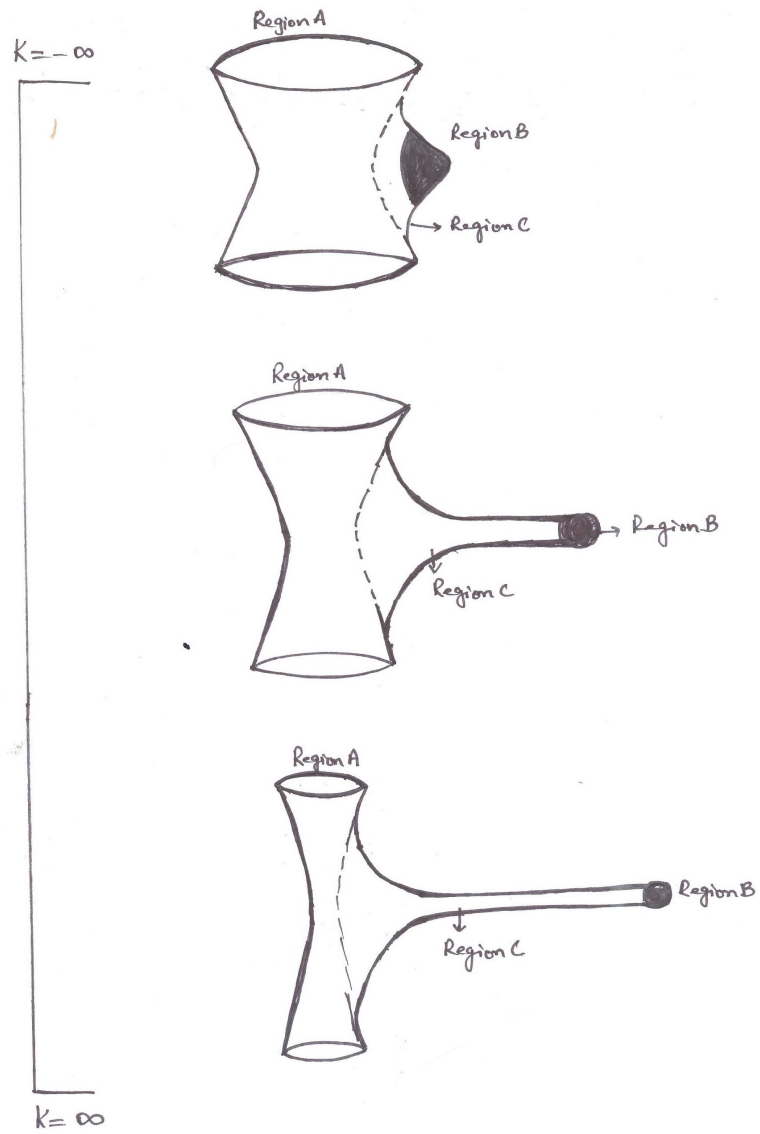


Figure 4.4: The variation of the size of Universe during the evolution of open Suture Model from Big Bang to Big Crunch.

4.2 Flat Suture Model

The flat Suture Model is constructed by considering a denser closed Friedmann Universe and a rarer compactified flat Friedmann Universe of same volume. A section of $1/N$ of the volume of denser Friedmann Universe is cut out and replaced by the rarer compactified flat Friedmann Universe such that the mass of the model remains the same. Both the regions are then joined together by the Schwarzschild geometry. The cut and paste view of the flat Suture Model is given in Figure 4.5 and 4.6. The flat Suture Model would follow the same requirements and the geometry as the Suture Model (section 3.2.1) except for the region B which corresponds to the hyper-cone structure for the flat Friedmann Universe. To limit the parameters, the transformations are given in Eq.(4.1) and Eq.(4.2). The metric for the flat Friedmann Universe in the compactified coordinates is given by

$$ds^2 = a^2(\eta')[\sec^2 \eta' d\eta'^2 - \sec^2 \chi' d\chi'^2 - \tan^2 \chi' (d\theta^2 + \sin^2 \theta d\phi^2)]. \quad (4.30)$$

The scale factor and the cosmic time in terms of compactified coordinates are

$$a(\eta') = \frac{a_o}{2} \tan^2 \eta', \quad (4.31)$$

$$t(\eta') = \frac{a_o}{6c} \tan^3 \eta'. \quad (4.32)$$

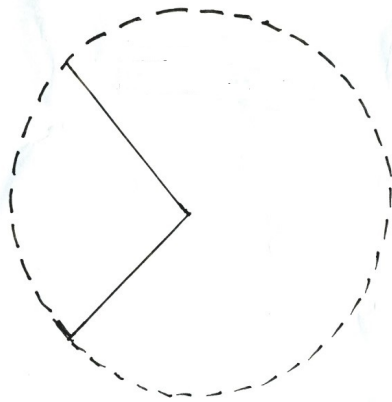
At $\eta' = 0$, $a(\eta') = 0$ and $t(\eta') = 0$ while at $\eta' = \frac{\pi}{2}$, $a(\eta')$ and $t(\eta')$ becomes infinite. From the point of an observer located in the region B, the evolution proceed normally for denser closed Friedmann Universe (region A) given by

$$ds^2 = a^2(\eta)[d\eta^2 - d\chi_{s''}^2 - \sin^2 \chi_{s''} (d\theta^2 + \sin^2 \theta d\phi^2)], \quad (4.33)$$

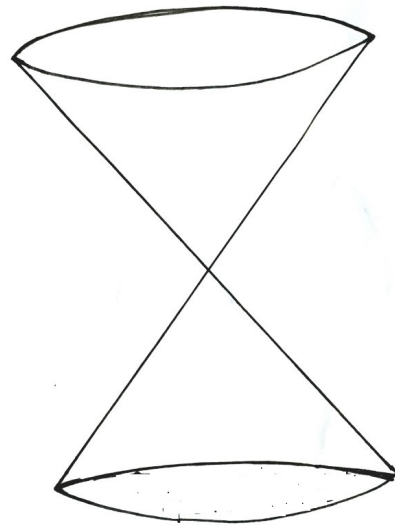
where, $\chi_{s''}$ represents the hyperspherical angle for this smaller region, varies from 0 to π , while η varies from 0 to 2π . The metric for the rarer flat Friedmann region in compactified coordinates is given by

$$ds^2 = a^2(\eta')[\sec^2 \eta' d\eta'^2 - \sec^2 \chi'_v d\chi'_v{}^2 - \tan^2 \chi'_v (d\theta^2 + \sin^2 \theta d\phi^2)]. \quad (4.34)$$

The radial parameter $\chi_{s''}$ goes from 0 at the center of region A to some χ_R at the junction with the Schwarzschild region. At the boundary $\chi_{s''}$ has to be constant over the entire evolution. The radial parameter χ'_v varies from some χ'_T at the junction with the Schwarzschild region to $\frac{\pi}{2}$ while the time parameter η' varies from 0 to $\frac{\pi}{2}$ as shown in Figure 4.7.



Denser closed
Friedmann Universe



Rarer flat
Friedmann Universe

Figure 4.5: The cut and paste view of the flat Suture Model with two dimension suppressed. The denser closed Friedmann Universe contains the hyperspherical angle $\chi_{s''}$, as the radial parameter, whereas $\chi_{l''}$, is the hyperspherical angle for the rarer flat Friedmann Universe.

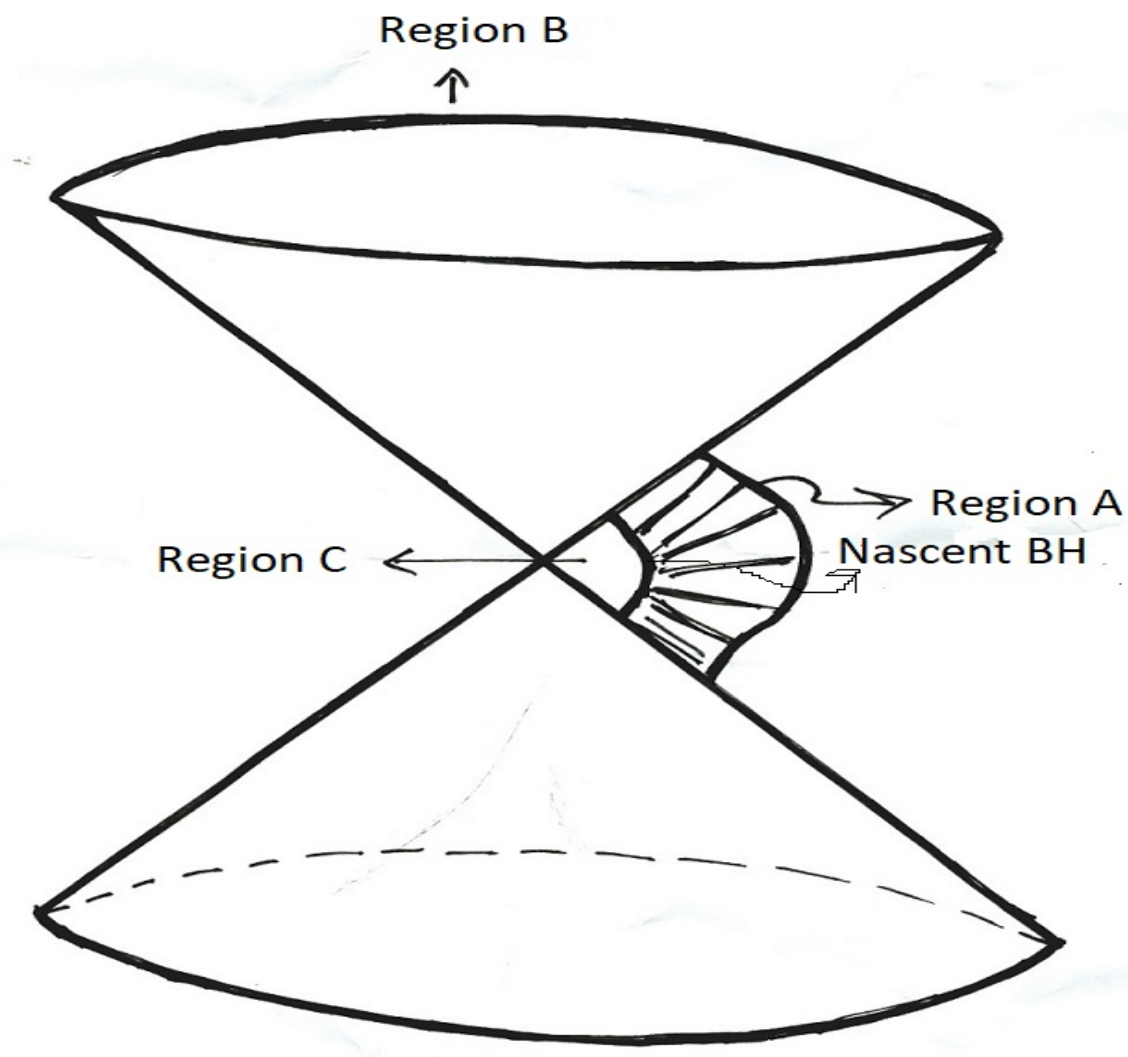


Figure 4.6: The cut and paste view of the flat Suture Model with two dimension suppressed.

Both the region start at the same time where $\eta = 0$, due to the difference in the densities of two Friedmann regions, the denser region evolves at a faster rate than the rarer one. Region A reached its phase of maximum expansion at $\eta = \pi$ earlier than region B, hence region A starts collapsing while region B is still expanding. Region B reaches its phase of maximum expansion at $\eta = \frac{\pi}{4}$, any observer at the boundary between region B and C can view region A as shrinking in size and collapsing in to a black hole and the rate of collapse actually slow downs near the Big Crunch. The mass of black hole formed is calculated and discussed in the following section.

4.2.1 Boundary Conditions for the Flat Suture Model

For the smooth evolution of the flat Suture Model from Big Bang to compactified end at $\eta' = \frac{\pi}{2}$, the boundary conditions as given below should be well defined for region A, B and C.

Boundary between Region A and C

The relation between the circumference and the radius of the Schwarzschild region at the boundary between region A and C is given by

$$C_{s''} = 2\pi R_{s''}, \quad (4.35)$$

where, $R_{s''}$ is the r value of the Schwarzschild region at the boundary between the regions A and C. The relation between the expansion factor and the Schwarzschild radius at the boundary between region A and C is given as

$$R_{s''} = a \sin \chi_{s''}. \quad (4.36)$$

Substituting this value in Eq.(4.35), we get

$$C_{s''} = 2\pi a \sin \chi_{s''}. \quad (4.37)$$

where,

$$a = \frac{a_{0_{s''}}}{2}(1 - \cos \eta), \quad (4.38)$$

Using Eq.(4.37), we get

$$C_{s''} = \pi[a_{0_{s''}} \sin \chi_s(1 - \cos \eta)]. \quad (4.39)$$

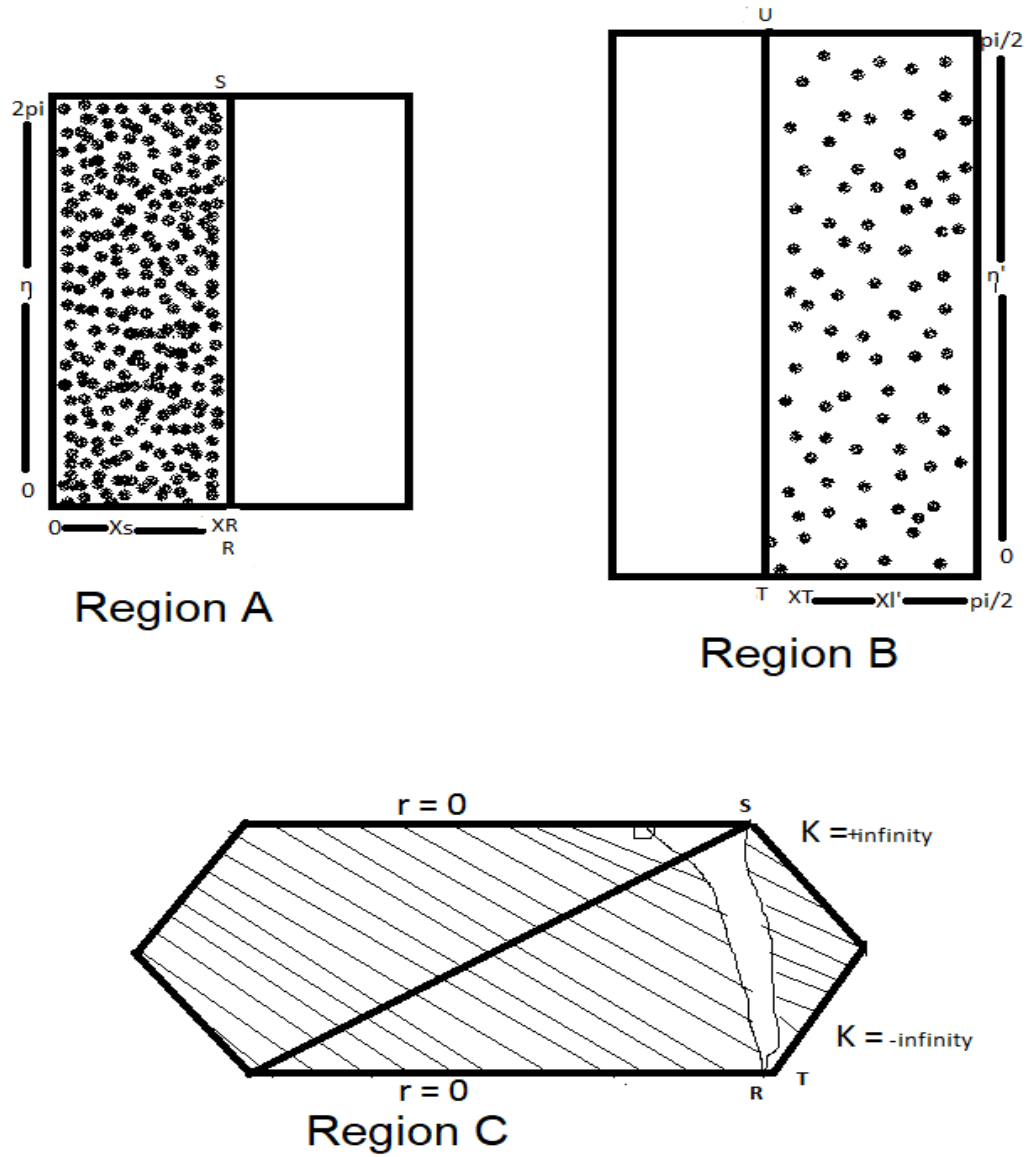


Figure 4.7: The CP diagram for the flat Suture Model. For region A, the time parameter η goes from 0 to 2π , while $\chi_{s''}$ varies from 0 to χ_R . In region B, η' varies from 0 to $\pi/2$ while $\chi_{l''}$ varies from χ'_T to $\pi/2$. In region C, the time parameter Φ goes from $-\pi/2$ to $\pi/2$ corresponding to the initial singularity to the final singularity at $r = 0$. The York time K goes from $-\infty$ to ∞ for these singularities.

Boundary between Region B and C

The relation between the circumference and the radius of the Schwarzschild region at the boundary between region B and C is given by

$$C_{l''} = 2\pi R_{l''}. \quad (4.40)$$

By the direct comparison of Schwarzschild and compactified flat Friedmann metric, the relation between the expansion factor and the Schwarzschild radius is given by

$$R_{l''} = a(\eta') \tan \chi'_{l''} \quad ; \quad 0 \leq \chi'_{l''} \leq \frac{\pi}{2}. \quad (4.41)$$

Substituting value of $R_{l''}$ in Eq.(4.40), we get

$$C_{l''} = 2\pi a(\eta') \tan \chi'_{l''}, \quad (4.42)$$

since,

$$a(\eta') = \frac{a_{0l''}}{2} \tan^2 \eta', \quad (4.43)$$

therefore Eq.(4.42) becomes

$$C_{l''} = \pi a_{0l''} \tan^2 \eta' \tan \chi'_{l''}. \quad (4.44)$$

4.2.2 Calculation of the Mass Discrepancy of the Flat Suture Model

Same assumption would be followed for the flat Suture Model. For definiteness, the density of the closed Friedmann region is taken to be 4 times the density of the compactified flat Friedmann region. The mass as seen from the boundary between region B and C can be calculated by using the boundary conditions. Comparing the metric given in Eq.(3.22) with the space-like section of flat Friedmann metric in compactified coordinates, we get

$$d\sigma^2 = a^2(\eta') \sec^2 \chi' d\chi'^2 \quad ; \quad R(\eta') = a(\eta') \tan \chi'. \quad (4.45)$$

Substituting the value of $d\sigma$ and dR in Eq.(3.23), we get

$$dw^2 = 0. \quad (4.46)$$

Slope of simultaneity associated with the world line of a particle in flat compactified Friedmann geometry is given by

$$\frac{dw}{dR} = 0. \quad (4.47)$$

Comparing Eq.(4.47) with Eq.(3.29), we get

$$\frac{c^2 R}{2Gm} = 1. \quad (4.48)$$

Therefore, the mass of a black hole as observed from the boundary between region B and C in flat Suture Model is given by

$$m = \frac{c^2 a(\eta')}{2G} \tan \chi_{l''}. \quad (4.49)$$

The mass as seen from the surface of a black hole is calculated in the section (3.2.4). It would be the same except for the notation, I have used for the denser closed Friedmann region, i.e.

$$m_{s''} = \frac{3}{4}(\chi_{s''} - \frac{1}{2} \sin 2\chi_{s''})a(\eta). \quad (4.50)$$

The mass expression obtained in Eq.(4.49) is in compactified coordinate while the mass expression in Eq.(4.50) is in terms of the original coordinates. In terms of the original time and angle coordinates, Eq.(4.49) becomes

$$m = \frac{a(\eta)c^2}{2G} \eta^2 \chi_{l''}. \quad (4.51)$$

Now, it is clear from the above equation that the mass as seen from the boundary of flat Friedmann region and the Schwarzschild region is dependent on η and χ which are the function of η' and χ' respectively, as given in Eq.(4.1) and Eq.(4.2). At $\eta' = 0$, the value of η becomes zero according to the transformation defined in Eq.(4.1). Putting $\eta = \eta' = 0$ in Eq.(4.50) and Eq.(4.51) implies the time of Big Bang where all the three regions merges together to a single point. Similarly, at $\chi' = 0$, the value of χ becomes zero according to the Eq.(4.2). Putting $\chi = \chi' = 0$ in Eq.(4.60) and Eq.(4.51), we get $m_{s'} = m = 0$. The difference between both the masses is significant when I match the upper limits of η and χ . At $\eta' = \frac{\pi}{2}$, the value of η becomes infinite. Putting this value in Eq.(4.51), the mass seen from the boundary

between flat Friedmann and the Schwarzschild region would be infinite. Same will be the case with $\chi' = \frac{\pi}{2}$. So, there is a clear difference of the mass as seen from the surface and the mass as seen from the boundary of region A and C in case of the flat Suture Model. Similar to the assumption I have made in open Suture Model, the mass discrepancy can be found out at a specific value, i.e. $\eta = \frac{\pi}{2}$. Therefore, Eq.(4.50) becomes

$$m_{s''} = \frac{3}{4}(\chi_{s''} - \frac{1}{2} \sin 2\chi_{s''}) \frac{a_0}{2}. \quad (4.52)$$

The expansion factor in terms of original coordinates at $\eta = \frac{\pi}{2}$ is given by

$$a(\eta) = \frac{a_0 \pi^2}{8}. \quad (4.53)$$

Substituting Eq.(4.53) in Eq.(4.51) and rearranging, we get

$$\frac{a_0}{2} = \frac{8mG}{\pi^2 c^2 \chi_{l''}}. \quad (4.54)$$

Substituting Eq.(4.54) in Eq.(4.52), we get

$$m_{s''} = \frac{3G}{c^2 \pi^2 \chi_{l''}} (2\chi_{s''} - \sin 2\chi_{s''}) m. \quad (4.55)$$

Thus, the mass discrepancy for flat Suture Model is given by

$$\frac{\delta m}{m} = 1 - \frac{3G}{c^2 \pi^2 \chi_{l''}} (2\chi_{s''} - \sin 2\chi_{s''}). \quad (4.56)$$

Chapter 5

Conclusion

In Chapter 3, there is a discussion about the physical and mathematical aspects of the Suture Model, its behavior during the last stages of crunch, the derivation of the expression for the mass of a black hole formed during the whole evolution of the model. The basic purpose of construction of the Suture Model was to investigate two things, the conjecture of Penrose and the behavior of the Friedmann Universes towards the final singularity. For this purpose, the Suture Model was K -foliated and the result was observed for different values of York-time. The variation of K was from $-\infty$ to $+\infty$. It had been observed that as K varies between the given limit, the distance between the two closed Friedmann regions increases and they started separating off. As a result, the proper distance between the two regions after expanding and then collapsing goes to infinity while the volume shrinks to zero. The suture, possessing the topology of the 2-sphere times a finite line segment develops into an ever-lengthening corridor in the final stages of crunch. This corridor typically lacks the geometric symmetry of a 2-sphere and dominates the crunch. Hence the conjecture was verified that the black hole singularity and the Big Crunch singularity are not different but basically, they are the same aspect of a big singularity. In other words, the black hole singularity is a part of a final cosmological singularity. Fig 3.8 illustrates the fact that as the model is K -foliated, the distance between the two regions increases. At $K = -\infty$, the model starts as a point (Big Bang) and develops into 2 regions joined by a small empty space (corridor). As K increases, the corridor rapidly increases in length $K = \infty$ the two regions collapses to two points while the length of the corridor becomes infinite. The second part of Penrose's Conjecture was that the simultaneity of the black hole singularity

and the conformal end of the Universe can also be imagined in a suitably conformally transformed open Universe. Following this part of the conjecture, I have tried to extend the Suture Model to the open and flat Suture Model by considering the geometries of flat and open Friedmann Universes. After reviewing the Suture Model thoroughly, I have followed the same procedure and developed the boundary conditions for the Extended Suture Models, which demonstrate the fact that the match is possible for all the values of η for both the boundaries between the 3 regions. It is assumed that both the Friedmann regions (closed and compactified open) started at $\eta = 0 = \eta'$ and start expanding. The denser closed Friedmann region reaches its phase of maximum expansion at $\eta = \pi/2$ while the rarer compactified open or flat Friedmann Universe at $\eta' = \pi/4$. Due to the difference of density, the closed Friedmann Universe collapses at a faster rate than the open compactified Friedmann Universe. Therefore, region A begins to collapse while region B is still expanding, ultimately region A collapses to a black hole and can be observed, if viewed from the boundary between Schwarzschild region and the compactified Friedmann Universe. The mass of this nascent black hole is evaluated in chapter 4 by using the boundary conditions for both the cases, which shows that there is a difference of mass as appear from the surface of black hole and from the boundary between region B and C. The difference is calculated in section (4.1.2) and (4.2.2) which depends on the value of χ for both the cases. It can be concluded that the mass discrepancy in the closed Suture Model is defined at the value of χ at the boundary between region B and C and the value of η at the phase of maximum expansion, therefore it is a constant. For the Extended Suture Models, since the phase of maximum expansion is not the same for region A and B, therefore this is not a possible choice for η , but the mass discrepancy is defined at the value of χ at the boundary. The point is that the mass discrepancy is not constant but depends on the value of η . For both the cases, the phase of their maximum expansion is not the same, i.e. it does not satisfy on a specific value of η so for definiteness, η is taken to be $\pi/2$ to find the mass discrepancy.

To verify the conjecture and to observe the behavior of the Extended Suture Model at the end of compactified spacetime, it must be foliated by the sequence of space-like hypersurfaces of constant mean extrinsic curvature. This work is not done yet, but it could be observed that like-wise the foliation of Suture Model, the variation of the Extended Suture Model might be observed at different values of York-time. Since this Foliation involves much effort and time, therefore I have limited my dissertation to the bound-

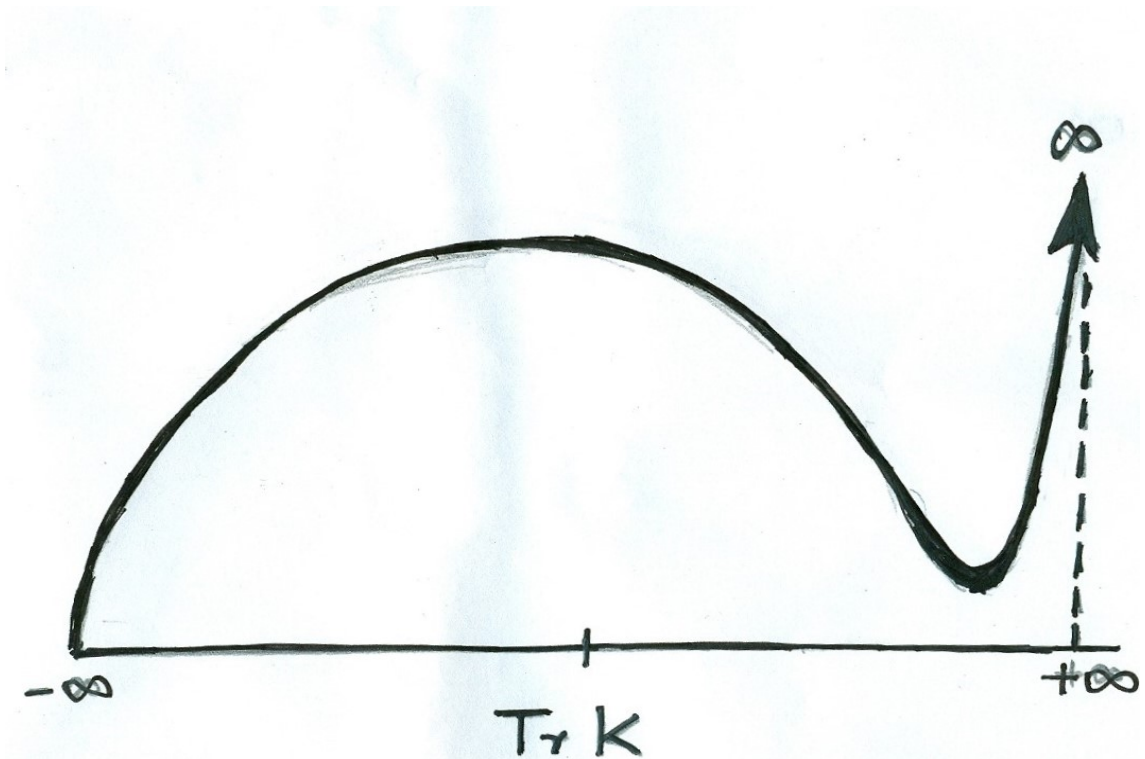


Figure 5.1: The plot between the TrK as it varies from $-\infty$ to ∞ and the distance is shown vertically depending on the crunch time.

ary conditions and the mass evaluation. It is assumed that the Extended Suture Model will behave like-wise the Suture Model, therefore we can make a hypothesis about the final stages, i.e. as the Extended Suture Model is K -Foliated with York time varying from $-\infty$ to ∞ , the distance between the two Friedmann regions increases while the volume decreases. At $\eta = 2\pi$ and $\eta' = \pi/2$ with $K = \infty$, the distance approaches infinity while volume shrinks to zero and the Schwarzschild region dominates over both the Friedmann regions, developing in to an ever-lengthening corridor.

Bibliography

- [1] N. Huggett, C. Hofer, *The Stanford Encyclopedia of Philosophy: Absolute and Relational Theories of Space and Motion*, Metaphysics Research Lab Stanford University, (2017).
- [2] J. M. Knudsen, P. G. Hjorth, *Elements of Newtonian Mechanics: Including Non-linear Dynamics*, Springer Science and Media Press, (2002).
- [3] A. Einstein, *Relativity: The Special and the General Theory*, Methuen and Co. Ltd, (1920).
- [4] R. L. Herman, “Simultaneity, Time Dilation and Length Contraction using Minkowski Diagrams and Lorentz Transformation”, *World Scientific*, (2008) 1-11.
- [5] A. Qadir, *Relativity: An Introduction To The Special Theory*, World Scientific Publishing Co. Pte. Ltd, (1989).
- [6] I. Newton, *Philosophiae Naturalis Principia Mathematica*, G.Brookman (1833).
- [7] J. D. Norton, “General Covariance and the Foundation of General Relativity: Eight Decades of Dispute”, *Rep. Prog. Phys.* **56** (1993) 791-858.
- [8] A. Qadir, *Einstein’s General Theory of Relativity*, (under preparation).
- [9] C. W. Misner, K. S. Throne, J. A. Wheeler, *Gravitation*, W. H. Freeman and Company, (1973).
- [10] C. Orchiston, I. Whittingham, “Michell, Laplace and the Origin of the Black Hole Concept”, *Journal of Astronomical History and Heritage.* **12** (2009) 90-96.

- [11] E. Poisson, *The Mathematics of Black Hole Mechanics*, Cambridge University Press, (2004).
- [12] A. S. Eddington, “A Comparison of Whitehead’s and Einstein’s Formulae”. *Nature* **113** (1924) 192-195.
- [13] D. Finkelstein, “Past-future asymmetry of the gravitational field of a point particle”, *Phy. Rev.* **110** (1958) 965-967.
- [14] M. S. Longair, *Confrontation of Cosmological Theories with Observational Data*, Springer Science and Business Media, (1974).
- [15] A. Qadir, J. A. Wheeler, “Black hole singularity as a part of big crunch singularity”, *Proceedings of the Fifth Marcel Grossman Meeting, World Scientific* **65** 404-410 (1981).
- [16] R. W. Lindquist, J. A. Wheeler, “Dynamics of a Lattice Universe by the Schwarzschild-Cell Method”, *Rev. Mod. Phy.* **29** (1957) 432-443.
- [17] A. Qadir, “Black hole in closed Universes”, *Proceedings of the Fifth Marcel Grossman Meeting, World Scientific* (1989) 593-624.
- [18] A. Qadir, J. A. Wheeler, “Late Stages of Crunch”, *Nuclear Physics B-Proceeding Supplements*, **6** (1989) 345-348.
- [19] D. R. Brill, J. M. Cavallo, J. A. Isenberg, “K-surfaces in the Schwarzschild spacetime and the construction of lattice cosmologies”, *Journal of Mathematical Physics*, **21** (2008) 2789-2796.
- [20] A. Qadir, “Length and volume of the Qadir-Wheeler suture model”, *Phys. Rev. D.* **63** (2001) 083502-083507.